# UNCLASSIFIED

## AD 271 636

*Reproduced*
*by the*

ARMED SERVICES TECHNICAL INFORMATION AGENCY
ARLINGTON HALL STATION
ARLINGTON 12, VIRGINIA

# UNCLASSIFIED

# WOODS HOLE OCEANOGRAPHIC INSTITUTION

Reference No. 62-2

Marine Meteorology

WATER VAPOR DISTRIBUTION

IN THE SUB-CLOUD TRADE WIND AREA
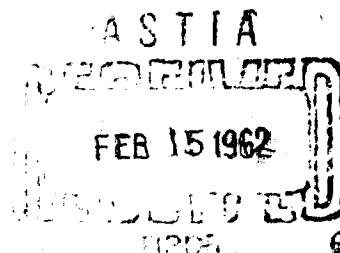
WOODS HOLE, MASSACHUSETTS

Woods Hole Oceanographic Institution

Woods Hole, Massachusetts

Reference No. 62 - 2

Marine Meteorology

Water Vapor Distribution in the Sub-Cloud

Trade Wind Air

by

Andrew F. Bunker

Technical Report #47

January 1962

APPROVED FOR DISTRIBUTION

Paul M. Fye, Director

# TABLE OF CONTENTS

# Water Vapor Distributions in the Sub-Cloud Trade Wind Air

## Abstract

Observations of the mixing ratio were made simultaneously at three levels in the sub-cloud layer of the trade wind east of the Bahama island of Eleuthera. Three airplanes were equipped with psychrographs capable of yielding significant 3-second averages of the mixing ratio. On 8 days, August 8 to 16, 1960 41 formation flights were made on east-west or north-south courses, giving 123 series of mixing ratios for analysis. Runs extended over 10 or 20 minutes and the levels were usually 400', 800', and 1200'. From these series the following statistical quantities have been computed: (a) the standard deviations of the mixing ratios at each level and of the height-averaged mixing ratio, (b) the correlation coefficients between the mixing ratios at different levels, (c) the average for each level, and (d) the spectral contributions of the height-averaged mixing ratio for all flights and a few contributions for individual levels. Standard deviations at individual levels varied from 1.10 to 0.15 g/kg while the height-averaged mixing ratio gave values from 0.56 to 0.14 g/kg. Correlation coefficients between the top of the layer to the bottom varied from 0.9 to 0.2. The spectral analyses of the different flights are similar in that they all show that roughly 75% of the variance of the mixing ratio is contributed by wavelengths longer than 3.75 km, and 22% by the wavelengths between 3.75 and 1 km. Only a few small peaks of variance appear at the shorter wavelengths. The observations and analyses were carried out partially as a check upon the hypothesis of Woodcock that orographic showers in the trade wind regions have their origin in moist parcels of air about 2 km in diameter. The contribution

to the standard deviation by the wavelengths from 1 to 3.75 km amounts to 0.14 g/kg. A differential temperature of 0.23°C would be generated by the condensation of the excess water vapor of the more moist parcels if the air mass is forced up a mountain slope. Such a temperature difference seems to be sufficient to start a shower. The data were analyzed also for relations between wind speed, cross-wind and parallel-wind differences and the correlation coefficient, standard deviations, and gradients. Only weak relations were noted.

# I Meteorological Background

Orographic trade wind shower cells are more likely to originate, according to Woodcock (1960), in the air parcels that are more humid than adjacent drier parcels. If the air is forced to ascend and condensation begins, the more moist parcels gain buoyancy before the drier parcels do, and hence have a greater probability of forming the nuclei of rain showers. After this proposal was brought forth it was asked whether the atmosphere does have a structure that could be described as containing relatively large parcels (1 or 2 km in diameter) extending throughout a large part of the sub-cloud layer with mixing ratios significantly in excess of the average. It was found that no data existed that would answer this question and hence a three-airplane expedition to the Bahama region of the trades was organized to study the horizontal and vertical moisture structure during an eight day period.

Observations of dry- and wet-bulb temperatures were made simultaneously at three levels during 10- or 20-minute flights upwind, downwind, and cross wind. The three airplanes were flown in a line tilted 45° forward of the vertical so that the pilots of the lower airplanes could guide on the upper airplane. See Figure 1. The work was done off the east shore of Eleuthera in the Bahamas where the trades were blowing with their usual variation in speed, stability, and cloud cover.

The data obtained were analyzed by computing averages, and standard deviations of mixing ratio, correlation coefficients between the simultaneous variations at the three levels, and standard deviations of the mixing ratios averaged individually over three levels. These quantities taken together give

a good but not complete description of the water vapor distribution and variation. Mixing ratio values were plotted on height-distance diagrams to give a visual impression of the grouping and extent of moist parcels. To further aid in the description of water vapor structure, power spectra were computed for the runs to define the scale of variation.

## II Observational Equipment and Procedure

### A. Psychrograph

The observations of dry- and wet-bulb temperatures that form the basis for the computation of the mixing ratios were obtained from thermistor bead psychrographs. Each bead formed the fourth leg of a Wheatstone Bridge so that their resistance may be measured and recorded. Calibration charts which relate these resistances to temperature were constructed from laboratory tests. One bead was covered with a wetted wick so that the wet-bulb temperature was given. The other bead was bare and yielded the dry-bulb temperature. In two of the airplanes a single bridge and recorder were used and the dry- and wet-thermistors were switched alternately into the bridge. On the other airplane two bridges and a double channel recorder were used so that continuous records of both wet and dry temperatures were obtained. On the R4D, the top aircraft, a previously built and described (Bunker and McCasland, 1954) psychrograph and Leeds and Northrup self-balancing potentiometer was used for recording data. On the other two airplanes, a Cessna 180 and a Heliocourier, a smaller simplified version of the same psychrograph was used. This version was built and calibrated by A.T. Spencer. No report has been written about its specifications. The data collected in the Cessna was recorded on an L & N small Speedomax while the data from the Heliocourier was recorded on a two-channel Varian.

The maximum probable errors of the thermistor psychrograph are about ±0.25°C when standard laboratory care and equipment are used: in calibrating the thermistors, in drawing calibration curves of the thermistors and bridges, in reading of the records, and in correction for dynamic heating of the beads by the motion of the airplane. A smaller error is attained in determining relative temperatures rather than absolute temperatures by comparisons of values taken from the three airplanes flying wing to wing. After correction of temperature to the mean obtained by the three, a relative probable error of about ±0.1 was obtained. On a few occasions wicks became dry and gave erroneous readings. These cases are recognizable if not noted at the time of occurrence and can be rejected and hence are not included in this accuracy definition.

B. Airplanes, Communications, and Procedures

The three airplanes were in radio contact to coordinate alignment of the airplanes and marking of the records. The time marking was accurate to about 1 second. An observer in the blister of the R4D coordinated all maneuvers, started all observing runs and called out times so that the other observers could mark their charts. The standard procedure was for the R4D to take the lead at 1200' (or 1500'), the Cessna to follow 400' below and 400' to the rear (or 500') while the Heliocourier trailed another 400' behind and below (or 500'). This formation was accomplished over the northern part of Eleuthera Island. When a good formation was attained, the line turned East and flew over the north Lighthouse which was always used as a basic reference point. See Figure 1. After flying 3 to 5 minutes upwind, depending on the wind speed, the signal for the beginning of the run was given and all charts marked accordingly. After the

10 (or 20) minute flight was completed a procedural turn was executed and a downwind run was started. After completion of the run the flight was continued past the shoreline, and a 270° turn through the south point to a cross-wind course was made. Again passing over the Lighthouse, a run was started a few minutes after passing the shore. Upon completion of the run another turn and another run was made cross-wind to the south. As an attempt was made to remain in the same air mass, the airplanes drifted downwind, a fact not shown in Figure 1.

### C. The Field Party and Laboratory Staff

The following members of the field party carried out the following tasks and responsibilities. Mr. Alfred Woodcock, Chief Scientist, was leader of the group and acted as observer in the Cessna 180. Mr. Claes Rooth aided in the planning of the flight and acted as coordinator and radio announcer in the R4D. Mr. Andrew Bunker operated the psychrograph in the R4D and was responsible for its calibration and the comparisons between the other psychrographs. Mr. Allard Spencer operated the psychrograph in the Heliocourier and built and calibrated the psychrographs in both the Heliocourier and the Cessna. Mr. Joseph Levine accompanied the expedition to make observations of the liquid water and vertical velocities in cumulus clouds. The R4D was flown by Capt. Norman Gingrass and his crew. The Cessna was flown by Mr. Bruce Larusso of the Sunny South Aviation Company. Mr. Robert Weeks piloted the Heliocourier.

All readings of records and reduction of data was done under the direction of Mr. Andrew Bunker. The programs for the Recomp II for computing mixing

ratios, temperatures, correlations and spectral analysis were written by
Mrs. Jacqueline Webster. After debugging these programs, Mrs. Webster
turned the work of reading the records and using the computer over to
Miss Carole Miller.

Mr. Claes Rooth has given much valuable help in the interpretation of the
data and in the scaling of the Malkus-Witt models to the present circumstances.

III Data Reduction Techniques

A. Measurement of Records

Psychrograph records were recorded on (1) 10-inch L & N charts, (2)
5-inch L & N charts, and (3) 5-inch Varian charts. The times of occurrances
of events were written or side marked on the charts by the observers who were
listening to the time and run announcements from the announcer flying in the
R4D. With this system all but a few runs were synchronized within a second of
time. The first step in the reading was the division of the records into the
proper three-second intervals. Next, the ink traces were read in units of the
chart paper and written on tabulating sheets. These values were entered into
the Recomp II machine and the values of the temperatures, mixing ratios,
potential temperatures, and densities were computed and typed. In addition to
the type-out, values of the mixing ratio were punched on tape for future use in
running correlations and auto-correlations.

B. Calibration of Chart Readings vs Temperature

The relation between the chart readings and the temperatures were expressed
as quadratic equations and the equation constants entered into the memory of
the Recomp II. Each instrument and each range has its own characteristic

constants. These constants were determined in the following manner. First a temperature-resistance curve for each thermistor was constructed using values obtained from measurements made within a thermally insulated calibration box. Next the relation of the chart displacement to resistance was determined for each psychrograph and range. This relation was then converted to a quadratic equation for entry into Recomp II. Frequent instrument sensitivity checks were made during the trip and new constants determined if any changes were found.

### C. Recomp II Psychrograph Program

Mrs. Jacqueline Webster programmed the Recomp II computing machine made by Autonetics Division of North American Aviation Corp. to convert chart readings to temperature and compute the following meteorological quantities from temperatures, pressures and dynamic heating corrections: dry-bulb temperatures, $T$; wet-bulb temperatures, $T_w$; mixing ratio, $q$; potential temperature, $\theta_d$; virtual temperature, $T_v$; potential virtual temperature, $\theta_v$; equivalent potential temperature, $\theta_e$; and density, $\rho$ . If a pressure-height relation is given, the program will interpolate heights for the given pressures.

The following equations were used to compute the various quantities:

$$e_s = 6.11 \times 10^{\frac{aT_w}{b+T_w}}, \qquad a = 7.5 \qquad (1)$$
$$b = 237.3$$

$$q_s = \frac{0.622\, e_s}{p-e_s}$$

$$q = q_s - \frac{T-T_w}{(L/C_{pd})}, \qquad \text{where } L = 595 - 0.5\, T_w$$
$$C_{pd} = 0.29$$

$$\theta_d = (T + 273.2) \left(\frac{1000}{p}\right)^K \qquad\qquad K = 0.286 \qquad (4)$$

$$T_v = (T + 273.2) \left(\frac{1+1.61q}{1+q}\right) \qquad\qquad (5)$$

$$\theta_v = T_v \left(\frac{1000}{p}\right)^K \qquad\qquad (6)$$

$$T_e = T_w + \frac{q_s L}{C_{pd}} \qquad\qquad (7)$$

$$\theta_e = (T_e + 273.2) \left(\frac{1000}{p}\right)^K \qquad\qquad (8)$$

The computer has two outputs of computations; the typewriter and the punched tape. All of the computed values described are typed out and the mixing ratios are punched out on the tape for later use in computing correlation coefficients. The write-out of temperatures, etc. can be abbreviated to only dry-bulb, wet-bulb temperatures and mixing ratios. This abbreviation is valuable at times since it requires a lot of computer time to print out the full set. A few of the runs in the present work were typed out completely. The rest of the series had complete write-outs only every tenth computation. Mixing ratios were always punched onto tapes.

D. Correlations, Deviations, Averages, and Auto-correlations

As mentioned in the introduction, it was desired to find some statistical parameter or parameters that could be used as an objective measure of the humidity structure to be compared with the requirements of the Woodcock concept of showers originating from particular sized humidity inhomogeneities. It was decided that the standard deviation, the correlation coefficient between

the mixing ratios at the three levels, and the standard and mean deviations of the height-averaged mixing ratio would give the best description of the humidity structure when all are considered together.

The program for computing correlations and standard deviations was furnished by the manufacturer of Recomp II. Computation of these quantities was completed easily by feeding the mixing ratio tapes for the three levels into the machine. The standard deviations of the height-averaged mixing ratio, $\sigma(q_{123})$ is also important for the final discussion. We note that:

$$\sigma_{q_{123}} = \sqrt{\overline{\left(\frac{q_1 + q_2 + q_3}{3}\right)^2}} = 1/3 \sqrt{\overline{q_1^2 + 2q_1 q_2 + 2q_1 q_3 + q_2^2 + 2q_2 q_3 + q_3^2}} \qquad (9)$$

but $\overline{q_1 q_2} = r_{1,2} \sigma_{q_1} \sigma_{q_2}$ and $\overline{q_2 q_3} = r_{2,3} \sigma_{q_2} \sigma_{q_3}$ etc. $\qquad (10)$

Hence

$$\sigma_{q_{123}} = 1/3 \sqrt{q_1^2 + q_2^2 + q_3^3 + 2r_{1,2} q_1 q_2 + 2r_{1,3} q_1 q_3 + 2r_{2,3} q_2 q_3} \qquad (11)$$

Values of $\sigma_{q_{123}}$ were computed from (11).

E. Spectral Analysis of Moisture Distributions

As the analysis of the data progressed it became evident that much information pertinent to the Woodcock hypothesis could be obtained by making spectral analyses of the mixing ratio distributions. Therefore Mrs. Webster wrote a program for the Recomp II, that would give the smoothed spectral power for either single-level runs or the height-averaged values. In constructing the program for this work the technique of Tukey was used as described by Blackman and Tukey (1958). The formula used is:

$$V_T = \Delta T \left[ C_o + 2 \sum_{q=1}^{m=1} C_q \cos \frac{qr\pi}{m} + C_m \cdot \cos r\pi \right] \qquad (12)$$

Smoothing was accomplished by weighting the spectral estimates as follows: 0.25, 0.5, 0.25.

IV  Pressure, Wind, Sea Temperature, and Water Vapor Distributions during the study period.

A.  Surface Pressure Patterns

The following synopsis of the surface pressure distributions has been made from weather maps drawn by the U.S. Weather Bureau at LaGuardia Airport, New York. This synopsis is considered sufficient to give the meteorological background for the study, hence a republication of the actual maps will not be made. All positions of the ridges and lows are expressed in relation to the observing area east of Eleuthera.

| August 8, 1960: | Eleuthera is south of a long pressure ridge; isobars quite straight; slight anticyclonic flow. |
| August 9, 1960: | Eleuthera south of small high center in long ridge; slight anticyclonic flow. |
| August 10, 1960: | Ridge still weakening; weak anticyclonic flow. |
| August 12, 1960: | Eleuthera west of ridge; cyclonic curvature of isobars to south of Eleuthera. |
| August 13, 1960: | Ridge intensified to north of Eleuthera; cyclonic flow to southeast. |
| August 14, 1960: | Ridge stronger to north; greater cyclonic flow to south. |

August 15, 1960:     Height pressure to north of Eleuthera; isobars with both

cyclonic and anticyclonic curvature.

August 16, 1960:     Definite wave southeast of Cuba with trough line extending

over Eleuthera.

August 17, 1960:     Low pressure center a few miles to the southeast of

Eleuthera.

B.  Winds

Average winds for each day were found by averaging the values obtained

from the following sources:  (1)  the Nassau Airport wind measurements; (2)

visual observations of the sea state during the flights, and (3) pilot balloon

observations made at Eleuthera, or San Salvadore, or Miami, if Eleuthera's

winds were not available.  Ship reports as plotted on the weather maps were

scanty and conflicting and hence were ignored.  Very good agreement was noted

among the three sets of observations that were used.  Table 4A presents these

values in knots.

Table 4A

Average Wind Speeds During Flights in Knots

| August 8, 1960 | 13.3 | August 12, 1960 | 7.7 |
|---|---|---|---|
| August 9, 1960 | 10.0 | August 13, 1960 | 8.4 |
| August 10, 1960 | 9.0 | August 14, 1960 | 16.0 |
| August 11, 1960 | 7.7 | August 16, 1960 | 11.5 |

Table 4B presents the wind shears as computed from the pilot balloon

observations.  Shears are expressed in meters per second per kilometer and

degrees per kilometer.

Table 4B

Wind Shears

| Date | Location | m/sec/km | °/km |
|------|----------|----------|------|
| August 8, 1960 | Eleuthera | -0.8 | 6 |
| August 9, 1960 | " | -0.3 | 8 |
| August 10, 1960 | " | -0.7 | - 3 |
| August 11, 1960 | " | -1.1 | - 2 |
| August 12, 1960 | " | 0.5 | - 6 |
| August 13, 1960 | San Salvadore | 1.8 | 18 |
| August 14, 1960 | " | 1.6 | 3 |
| August 16, 1960 | Miami | 5.3 | 3 |

C. Sea Temperatures

Sea temperatures were read from the table of marine data contained in the Northern Hemisphere Data Tabulation of the U.S. Weather Bureau and plotted on a chart of the area. Since data are scarce, all data from August 8 to August 16, 1960 were plotted in Figure 2. It is seen that both the north-south and east-west temperature gradients were very slight. All values found lay between 82 and 88°F with 3/4's of them 84, 85, or 86°F. The water deepens very rapidly to the east of Eleuthera so no warming due to shallow water heating is thought to be present in the flight areas.

V. Data Presentation

A. Graphical Presentation

All data obtained on these flights have been plotted on charts of height versus time or distance from the starting point. Because of drafting costs, only a few samples are reproduced here. These few have been chosen on the basis of high or low variability and high or low correlations between the values at the different levels. Figure 3 presents Run No. 1 of August 11, 1960 as a case of low variability as indicated by a low value of the root-mean-square of

of the mixing ratios, while Run No. 3 of August 9, 1960, is an example of high variability. Figure 4 presents Run No. 6 of August 10, having a very low correlation between the water vapor fluctuations at the three levels, while Run No. 8, August 11, has a high correlation. In Figure 5, Run No. 7, August 8, 1960 represents an example of negative correlations, while Run No. 4, August 11, shows the unusual sinusoidal waves in the lower levels and regular waves of much greater amplitude at the higher level.

B. Tabular Presentation of Statistical Data

The following tables have been set up to present values of (1) the standard deviations of the mixing ratio series, (2) the correlation coefficients (3) the average mixing ratios, and (4) other supplementary data pertaining to the flight courses, observation points and cloud amounts. The tables are set up with date, time of day, and the sky coverage by cumulus clouds, entered across the top. The second row gives the column headings for the direction of the flight, number of observation points used in the computation, average mixing ratio, standard deviations, and correlation coefficients. The numerical subscripts refer to the level at which the observations were taken. They are defined as follows:

    (1)   R4D level       1200 or 1500 feet

    (2)   Cessna level    800 or 1000 feet

    (3)   Heliocourier    400 or 500 feet

## Tabulation of Mixing Ratio and Supplementary Statistics

### Table 5A

August 8, 1960            Morning Runs            Cumulus Cloud Cover: 5/10

| Run | Height Feet | Direction $^\circ M$ | Obs. Points N | Average $\bar{q}$ g/kg | Standard Deviations $\sigma q$ | $\sigma q_{123}$ | Correlation Coefficients $r_{1,2}$ | $r_{2,3}$ | $r_{1,3}$ |
|---|---|---|---|---|---|---|---|---|---|
| 1 | 1500 | 090 | 174 | 17.89 | 0.36 | | | | |
| 1 | 1000 | " | " | 19.06 | 0.18 | 0.18 | 0.28 | 0.57 | -0.15 |
| 1 | 500 | " | " | 19.41 | 0.25 | | | | |
| 4 | 1500 | 270 | 200 | 17.94 | 0.51 | | | | |
| 4 | 1000 | " | " | 18.82 | 0.25 | 0.32 | 0.72 | 0.77 | 0.54 |
| 4 | 500 | " | " | 19.24 | 0.26 | | | | |
| 5 | 1500 | 090 | 200 | 17.98 | 0.37 | | | | |
| 5 | 1000 | " | " | 18.74 | 0.21 | 0.22 | 0.65 | 0.69 | 0.54 |
| 5 | 500 | " | " | 19.01 | 0.19 | | | | |
| 6 | 1500 | 270 | 200 | 18.00 | 0.29 | | | | |
| 6 | 1000 | " | " | 18.77 | 0.15 | 0.62 | 0.62 | 0.44 | 0.20 |
| 6 | 500 | " | " | 19.27 | 0.26 | | | | |

### Table 5B

August 8, 1960            Afternoon Runs            Cumulus Cloud Cover: 5/10

| Run | Height Feet | Direction $^\circ M$ | Obs. Points N | Average $\bar{q}$ g/kg | Standard Deviations $\sigma q$ | $\sigma q_{123}$ | Correlation Coefficients $r_{1,2}$ | $r_{2,3}$ | $r_{1,3}$ |
|---|---|---|---|---|---|---|---|---|---|
| 7 | 1500 | 090 | 200 | 16.77 | 0.43 | | | | |
| 7 | 1000 | " | " | 17.74 | 0.26 | 0.20 | 0.49 | -0.23 | -0.23 |
| 7 | 500 | " | " | 18.13 | 0.33 | | | | |
| 8 | 1500 | 270 | 200 | 17.10 | 0.34 | | | | |
| 8 | 1000 | " | " | 18.02 | 0.21 | 0.22 | 0.50 | 0.31 | 0.19 |
| 8 | 500 | " | " | 18.49 | 0.33 | | | | |
| 9 | 1500 | 090 | 200 | 16.76 | 0.44 | | | | |
| 9 | 1000 | " | " | 17.66 | 0.22 | 0.29 | 0.72 | 0.78 | 0.66 |
| 9 | 500 | " | " | 17.97 | 0.31 | | | | |
| 10 | 1500 | 270 | 200 | 16.93 | 0.48 | | | | |
| 10 | 1000 | " | " | 17.75 | 0.27 | 0.31 | 0.60 | 0.76 | 0.65 |
| 10 | 500 | " | " | 18.28 | 0.31 | | | | |

## Tabulation of Mixing Ratio and Supplementary Statistics

### Table 5C

August 9, 1960          Midday          Cumulus Cloud Cover: 4/

| Run | Height | Direct-ion $^\circ M$ | Obs. Points N | Average $\bar{q}$ g/kg | Standard Deviations | | Correlation Coefficients | | |
|-----|--------|------|------|------|------|------|------|------|------|
| | | | | | $q$ | $q_{123}$ | $r_{1,2}$ | $r_{2,3}$ | $r_{1,3}$ |
| 1 | 1500 | 090 | 200 | 16.66 | 0.78 | | | | |
| 1 | 1000 | " | " | 17.91 | 0.32 | 0.30 | -0.09 | 0.26 | 0.33 |
| 1 | 500 | " | " | 18.16 | 0.18 | | | | |
| 2 | 1500 | 270 | 200 | 16.84 | 0.52 | | | | |
| 2 | 1000 | " | " | 18.03 | 0.21 | 0.31 | 0.26 | 0.75 | 0.09 |
| 2 | 500 | " | " | 18.22 | 0.18 | | | | |
| 3 | 1500 | 000 | 200 | 16.73 | 1.10 | | | | |
| 3 | 1000 | " | " | 18.04 | 0.42 | 0.56 | 0.63 | 0.86 | 0.55 |
| 3 | 500 | " | " | 18.37 | 0.39 | | | | |
| 4 | 1500 | 180 | 200 | 17.19 | 0.59 | | | | |
| 4 | 1000 | " | " | 18.07 | 0.35 | 0.34 | 0.46 | 0.75 | 0.36 |
| 4 | 500 | " | " | 18.36 | 0.31 | | | | |
| 5 | 1500 | 090 | 200 | 17.67 | 0.42 | | | | |
| 5 | 1000 | " | " | 18.59 | 0.31 | 0.34 | 0.90 | 0.92 | 0.87 |
| 5 | 500 | " | " | 18.18 | 0.34 | | | | |
| 6 | 1500 | 270 | 200 | 17.74 | 0.36 | | | | |
| 6 | 1000 | " | " | 18.49 | 0.30 | 0.32 | 0.78 | 0.82 | 0.80 |
| 6 | 500 | " | " | 18.22 | 0.35 | | | | |

## Tabulation of Mixing Ratio and Supplementary Statistics

### Table 5D

August 10, 1960          Midday Runs          Cumulus Cloud Cover: 2/10

| Run | Height Feet | Direction $^{\circ}M$ | Obs. Points N | Average $\bar{q}$ g/kg | Standard Deviations $\sigma q$ | $\sigma q_{123}$ | Correlation Coefficients $r_{1,2}$ | $r_{2,3}$ | $r_{1,3}$ |
|---|---|---|---|---|---|---|---|---|---|
| 2 | 1500 | 295 | 180 | 16.70 | 0.81 | | | | |
| 2 | 1000 | " | " | 18.04 | 0.33 | 0.45 | 0.67 | 0.88 | 0.69 |
| 2 | 500 | " | " | 18.37 | 0.33 | | | | |
| 3 | 1500 | 030 | 200 | 16.80 | 0.61 | | | | |
| 3 | 1000 | " | " | 17.78 | 0.19 | 0.26 | 0.25 | 0.80 | 0.17 |
| 3 | 500 | " | " | 18.03 | 0.22 | | | | |
| 4 | 1500 | 220 | 200 | 16.83 | 0.58 | | | | |
| 4 | 1000 | " | " | 17.84 | 0.21 | 0.28 | 0.49 | 0.67 | 0.39 |
| 4 | 500 | " | " | 17.79 | 0.23 | | | | |
| 5 | 1500 | 100 | 200 | 17.42 | 0.54 | | | | |
| 5 | 1000 | " | " | 18.23 | 0.25 | 0.32 | 0.54 | 0.87 | 0.44 |
| 5 | 500 | " | " | 18.51 | 0.32 | | | | |
| 6 | 1500 | 280 | 200 | 17.21 | 0.48 | | | | |
| 6 | 1000 | " | " | 18.23 | 0.22 | 0.23 | 0.07 | 0.72 | -0.06 |
| 6 | 500 | " | " | 18.43 | 0.31 | | | | |
| 7 | 1500 | 010 | 200 | 16.38 | 0.56 | | | | |
| 7 | 1000 | " | " | 17.64 | 0.25 | 0.27 | 0.27 | 0.71 | 0.16 |
| 7 | 500 | " | " | 17.42 | 0.27 | | | | |
| 8 | 1500 | 190 | 260 | 16.39 | 0.64 | | | | |
| 8 | 1000 | " | " | 17.65 | 0.30 | 0.36 | 0.49 | 0.80 | 0.42 |
| 8 | 500 | " | " | 17.36 | 0.35 | | | | |

## Tabulation of Mixing Ratio and Supplementary Statistics

### Table 5E

| August 11, 1960 | | | Midday Runs | | | Cumulus Cloud Cover: 3/10 | | |

| Run | Height Feet | Direction $^\circ$M | Obs. Points N | Average $\bar{q}$ g/kg | Standard Deviations $\sigma q$ | $\sigma q_{123}$ | Correlation Coefficients $r_{1,2}$ | $r_{2,3}$ | $r_{1,3}$ |
|---|---|---|---|---|---|---|---|---|---|
| 1 | 1200 | 100 | 200 | 17.57 | 0.23 | | | | |
| 1 | 800 | " | " | 17.08 | 0.16 | 0.14 | 0.33 | 0.61 | 0.26 |
| 1 | 400 | " | " | 18.04 | 0.16 | | | | |
| 2 | 1200 | 290 | 200 | 17.43 | 0.24 | | | | |
| 2 | 800 | " | " | 16.96 | 0.18 | 0.17 | 0.59 | 0.60 | 0.56 |
| 2 | 400 | " | " | 17.90 | 0.19 | | | | |
| 3 | 1200 | 010 | 200 | 16.96 | 0.61 | | | | |
| 3 | 800 | " | " | 17.30 | 0.46 | 0.47 | 0.76 | 0.80 | 0.65 |
| 3 | 400 | " | " | 18.33 | 0.47 | | | | |
| 4 | 1200 | 200 | 200 | 16.87 | 0.65 | | | | |
| 4 | 800 | " | " | 17.32 | 0.43 | 0.47 | 0.77 | 0.94 | 0.74 |
| 4 | 400 | " | " | 18.39 | 0.45 | | | | |
| 5 | 1200 | 100 | 200 | 17.60 | 0.27 | | | | |
| 5 | 800 | " | " | 17.53 | 0.21 | 0.19 | 0.62 | 0.61 | 0.64 |
| 5 | 400 | " | " | 18.32 | 0.21 | | | | |
| 6 | 1200 | 280 | 200 | 17.58 | 0.33 | | | | |
| 6 | 800 | " | " | 17.53 | 0.23 | 0.23 | 0.67 | 0.73 | 0.52 |
| 6 | 400 | " | " | 18.39 | 0.24 | | | | |
| 7 | 1200 | 010 | 160 | 17.11 | 0.39 | | | | |
| 7 | 800 | " | " | 17.03 | 0.34 | 0.34 | 0.79 | 0.88 | 0.72 |
| 7 | 400 | " | " | 17.89 | 0.37 | | | | |
| 8 | 1200 | 190 | 200 | 17.25 | 0.47 | | | | |
| 8 | 800 | " | " | 17.12 | 0.39 | 0.41 | 0.84 | 0.94 | 0.83 |
| 8 | 400 | " | " | 17.96 | 0.44 | | | | |

## Tabulation of Mixing Ratio and Supplementary Statistics

### Table 5F

August 12, 1960          Midday Runs          Cumulus Cloud Cover: 2/10

| Run | Height Feet | Direction $^\circ M$ | Obs. Points N | Average $\bar{q}$ g/kg | Standard Deviations $q$ | $q_{123}$ | Correlation Coefficients $r_{1,2}$ | $r_{2,3}$ | $r_{1,3}$ |
|---|---|---|---|---|---|---|---|---|---|
| 3 | 1200 | 350 | 400 | 17.47 | 0.30 | | | | |
| 3 | 800 | " | " | 17.81 | 0.37 | 0.24 | 0.32 | 0.41 | 0.44 |
| 3 | 400 | " | " | 18.54 | 0.27 | | | | |
| 4 | 1200 | 180 | 400 | 17.42 | 0.35 | | | | |
| 4 | 800 | " | " | 17.76 | 0.23 | 0.24 | 0.49 | 0.83 | 0.48 |
| 4 | 400 | " | " | 18.60 | 0.26 | | | | |

### Table 5G

August 13, 1960          Midday Runs          Cumulus Cloud Cover: 2/10

| Run | Height Feet | Direction $^\circ M$ | Obs. Points N | Average $\bar{q}$ g/kg | Standard Deviations $q$ | $q_{123}$ | Correlation Coefficients $r_{1,2}$ | $r_{2,3}$ | $r_{1,3}$ |
|---|---|---|---|---|---|---|---|---|---|
| 2 | 1200 | 280 | 360 | 17.56 | 0.44 | | | | |
| 2 | 800 | " | " | 17.54 | 0.36 | 0.46 | 0.77 | 0.81 | 0.79 |
| 2 | 400 | " | " | 17.97 | 0.68 | | | | |
| 3 | 1200 | 010 | 400 | 17.16 | 0.29 | | | | |
| 3 | 800 | " | " | 16.92 | 0.25 | 0.26 | 0.64 | 0.68 | 0.47 |
| 3 | 400 | " | " | 17.54 | 0.36 | | | | |

### Table 5H

August 14, 1960          Midday Runs          Cumulus Cloud Cover: 2/10

| Run | Height Feet | Direction $^\circ M$ | Obs. Points N | Average $\bar{q}$ g/kg | Standard Deviations $q$ | $q_{123}$ | Correlation Coefficients $r_{1,2}$ | $r_{2,3}$ | $r_{1,3}$ |
|---|---|---|---|---|---|---|---|---|---|
| 1 | 1200 | 090 | 200 | 18.21 | 0.42 | | | | |
| 1 | 800 | " | " | 17.55 | 0.28 | 0.30 | 0.73 | 0.71 | 0.55 |
| 1 | 400 | " | " | 17.81 | 0.31 | | | | |
| 2 | 1200 | 270 | 200 | 18.13 | 0.33 | | | | |
| 2 | 800 | " | " | 17.60 | 0.26 | 0.30 | 0.63 | 0.83 | 0.51 |
| 2 | 400 | " | " | 17.92 | 0.42 | | | | |
| 3 | 1200 | 360 | 200 | 18.44 | 0.37 | | | | |
| 3 | 800 | " | " | 17.82 | 0.33 | 0.30 | 0.55 | 0.86 | 0.48 |
| 3 | 400 | " | " | 18.21 | 0.35 | | | | |
| 4 | 1200 | 180 | 200 | 18.33 | 0.43 | | | | |
| 4 | 800 | " | " | 17.77 | 0.43 | 0.33 | 0.61 | 0.66 | 0.29 |
| 4 | 400 | " | " | 18.19 | 0.35 | | | | |

## Tabulation of Mixing Ratio and Supplementary Statistics

### Table 5I

August 16, 1960                    Midday Runs                    Cumulus Cloud Cover: 7/10

| Run | Height Feet | Direction $^\circ$ M | Obs. Points N | Average $\overline{q}$ g/kg | Standard Deviation $\sigma q$ | $\sigma q_{123}$ | Correlation Coefficients $r_{1,2}$ | $r_{2,3}$ | $r_{1,3}$ |
|-----|-------------|-----------|------|---------|------|------|------|------|------|
| 1 | 1200 | 090 | 280 | 18.57 | 0.50 | | | | |
| 1 | 800 | " | " | 17.92 | 0.43 | 0.38 | 0.34 | 0.71 | 0.21 |
| 1 | 400 | " | " | 17.86 | 0.44 | | | | |
| | | | | | | | | | |
| 2 | 1200 | 280 | 200 | 18.70 | 0.32 | | | | |
| 2 | 800 | " | " | 17.87 | 0.21 | 0.21 | 0.44 | 0.62 | 0.46 |
| 2 | 400 | " | " | 18.26 | 0.26 | | | | |
| | | | | | | | | | |
| 3 | 1200 | 360 | 200 | 18.06 | 0.31 | | | | |
| 3 | 800 | " | " | 17.18 | 0.32 | 0.29 | 0.46 | 0.86 | 0.44 |
| 3 | 400 | " | " | 17.58 | 0.40 | | | | |
| | | | | | | | | | |
| 4 | 1200 | 180 | 180 | 17.91 | 0.35 | | | | |
| 4 | 800 | " | " | 17.20 | 0.29 | 0.26 | 0.46 | 0.76 | 0.39 |
| 4 | 400 | " | " | 17.42 | 0.31 | | | | |

## VI. Analysis of Data and Discussion

The data presented in Section V is analyzed now principally from the point of view of the Woodcock orographic shower concept, but also, a search is made for empirical relations between the various statistical parameters and the wind speed and flight course and height.

### A. Effect of Airplane Alignment upon the Data

In section 2 it was stated that the airplanes were aligned not vertically but rather along a line tilted 45° forward. This configuration was decided upon for the benefit of the pilots because it was thought that the data would not be adversely influenced. It is possible to test the influence of this or any other alignment of the airplanes by computing correlation coefficients with the values at one level advanced or retarded in relation to the other level. This has been done for several runs and several values of displacement. Figure 6 presents the computed coefficient for various lags. Zero lag corresponds to 45° forward tilt. A lag of 1 at the middle level and 2 lags at the top level corresponds to a vertical alignment. Two and 4 lags, 3 and 6 lags, and 4 and 8 lags correspond to 45°, 63°, and 71° backward tilt, respectively. It is seen that for correlation coefficients greater than 0.4 the effect of various tilts is to first increase the coefficient slightly and then to slightly decrease it. In the case of negative correlations the effect of changing alignment is to increase the coefficient markedly and transform the relation into a positive one but still with a very low coefficient.

During the first few days of operation the flight formation was very irregular due to the mis-match of optimum cruising speeds of the airplanes and lack of experience in scientific formation flying. As a result the lower airplane

sometimes lagged far behind the upper airplane, producing what appears to be ficticiously low correlation coefficients. As a test of this inexperience effect the range of observed coefficients of a given day were plotted against calendar date. Figure 7 shows that the range of values steadily decreases to values around 0.2. The large range during the earlier flights is suspected to be the result of poor formation flying rather than a true change in the vertical inhomogeneity of the air.

B. Vertical Gradients of the Mixing Ratio, q, and Standard Deviation $\sigma_q$

    1. Mixing Ratio

The daily averages of q at the 1500', 1000', and 500' levels or the 1200', 800' and 400' levels are presented in Table 6A. These are the averages of all runs made on a particular day.

Table 6A

Daily Averages of Mixing Ratio, q, and $\sigma_{q_{123}}$, at different levels expressed in g/kg

| Height | 1500' | 1000' | 500' | $\sigma_{q_{123}}$ |
|---|---|---|---|---|
| August 8 | 17.42 | 18.32 | 18.73 | 0.24 |
| August 9 | 17.14 | 18.19 | 18.25 | 0.36 |
| August 10 | 16.82 | 17.92 | 17.99 | 0.31 |
| Height | 1200' | 800' | 400' | $\sigma_{q_{123}}$ |
| August 11 | 17.30 | 17.23 | 18.15 | 0.30 |
| August 12 | 17.45 | 17.79 | 18.57 | 0.24 |
| August 13 | 17.36 | 17.23 | 17.75 | 0.34 |
| August 14 | 18.30 | 17.69 | 18.03 | 0.31 |
| August 16 | 18.31 | 17.52 | 17.78 | 0.29 |
| Level Average | 17.51 | 17.74 | 18.16 | |
| Average of all levels ------------ 17.80 --------------- | | | | 0.30 |

The gradient is seen to be negative on the average, but a puzzling minimum value of the mixing ratio developed at the 800' level during the latter part of the period. On the 8th, 9th, and 10th the gradient was negative at all levels and showed a daily progressive drying out of the air. On the 11th a very slight minimum developed at 800' but it disappeared on the 12th. On the 13th, 14th, and 16th very well defined minima occurred at the 800' level. The possibility of an instrument malfunction was ruled out by soundings made with the R4D psychrograph between 400' and 2500'. Mixing ratios measured with this single psychrograph confirmed the existence of the minima.

In looking for an explanation of this phenomenon various parameters were examined for day-to-day differences. Shower activity was not related to the moisture inversion since no showers occurred on the 14th while many were present on the 16th.

The shear in the wind direction was not related to the moisture inversion but it was noted that on the days with a moisture inversion the wind speed increased with height whereas on the days with a negative gradient of mixing ratio there was a negative shear. Thus it was possible that the phenomenon can be explained as an advection effect with more moist air being brought in at higher levels. The source of the more moist air is unknown.

It will be recalled that previous occurrences of mixing ratio inversions have been observed in the trade winds. Bunker, et al. (1949) noted that eight out of 29 days had zero or positive mixing ratio gradients when the gradients were computed for the entire sub-cloud layer. As a further test, the data were divided into 300' height groups, and the mixing ratios in each group computed using all of the data contained in the quoted paper. These averages showed a

slight minimum in the 900' to 1200' layer. Thus it would seem that a minimum instead of being an extraordinary event is rather common. Malkus (1958) noted differences in the lapse rate of the mixing ratio between two periods of high and low wind velocity of the trade winds. In the period of high winds (9.1 m/sec) gradients are smaller than in the period of low winds (5.7 m/sec). As the winds during the present Bahama study were low (4.8 m/sec average) one would expect steep negative gradients of the mixing ratio, and indeed a steep negative gradient $(-22 \times 10^{-9} \ cm^{-1})$ is found. This value agrees closely with the gradient observed in 1953 with low winds. The existence of minima during a period of steep negative gradients is even more puzzling unless a mechanism is found which acts to accumulate water vapor in the higher levels of the mixed layer. Two speculations may be made. One is that cloud drops settle down into the mixed layer and evaporate. This mechanism would furnish a supply of water vapor to the top of the layer. Another mechanism could be the spreading out of moist air at the base of the slight stable layer topping the turbulent layer of the trades. If air rises from a layer close to the sea surface and spreads out at the stable layer, then a negative gradient could be maintained as the air flows along filling up with water vapor.

Table 6B gives a more detailed breakdown of the observed gradients of the mixing ratio. The most interesting feature of this table is the positive gradients existing in the 800' to 1200' range.

## Table 6B

### Table of Mixing Ratio Gradients in g/g/cm

| Height Range | 1500'-1000' | 1000'-500' |
|---|---|---|
| August 8 | $-59.1\times10^{-9}$ | $-27.3\times10^{-9}$ |
| 9 | $-79.3$ " | $-4.0$ " |
| 10 | $-72.2$ " | $-4.6$ " |
| Average | $-70.2\times10^{-9}$ | $-12.0\times10^{-9}$ |

| Height Range | 1200'-800' | 800'-400' |
|---|---|---|
| August 11 | $5.8\times10^{-9}$ | $-75.8\times10^{-9}$ |
| 12 | $-27.9$ " | $-64.0$ " |
| 13 | $10.7$ " | $-42.7$ " |
| 14 | $50.0$ " | $-27.9$ " |
| 16 | $64.8$ " | $-21.3$ " |
| Average | $20.7\times10^{-9}$ | $-46.3\times10^{-9}$ |

2. Standard Deviations of the Mixing Ratio

Averages of the mixing ratio have been found and are tabulated in Table 6C.

### Table 6C

### Average Standard Deviations of Mixing Ratio in grams per kilogram

| Set 1 | | Set 2 | |
|---|---|---|---|
| Height in feet | $\sigma_q$ | Height in feet | $\sigma_q$ |
| 1500 | 0.53 | 1200 | 0.38 |
| 1000 | 0.26 | 800 | 0.31 |
| 500 | 0.29 | 400 | 0.35 |

The data has been separated into two sets of data since they represent height intervals. Both groups show a minimum at the middle height level. This variation can be explained as the result of a dry air mass covering the sub-cloud air and a more moist layer of air in contact with the water, for near the lower boundary. The mixing ratio gradients are steep at the top and bottom

of the layer due to weak small scale mixing at these levels. When dry air from aloft is forced into the lower air by the action of large scale turbulence or condensation convection large variations of the mixing ratio are produced at the top of the layer and smaller variations deeper in the layer due to small scale mixing of water vapor into the dry eddy. Similar mixing of the moist air from below produces large variations where the gradient is steepest and smaller variations deeper in the air mass.

3. Skewness of Mixing Ratio Distributions

Casual inspection of the mixing ratio cross sections, Figures 3, 4, and 5 shows that negative deviations from the average are greater than the positive deviations. Or, in other words, the distribution is not normal, but highly skewed. The reason for this skewness is the same as that for the variation of the standard deviation with height already discussed. The air mass of the cloud layer is many mixing ratio units drier than the turbulent sub-cloud layer while the air mass of the lowest meter is only slightly more moist. Thus down drafts being very dry air into the layer while updrafts lift only slightly more moist air.

The value of the skewness has been computed for only the August 9, 1960 north-bound Run No. 3. These values are -0.93 at 1500', -0.50 at 1000', and -1.0 at 500'. Figure 8 gives the histograms for the three levels of Run No. 3 and shows the long tail on the dry side and the sharp cut-off on the moist side. Figure 9 presents a histogram of the mixing ratio values observed during Run No. 2, August 16, 1960. As noted earlier a mixing ratio minimum developed in the sub-cloud layer. As a result of more moist air being present aloft only a few, weak, dry air intrusions occur. The absence of these intrusions preclude the production of a long tail of dry air and the great skewness of the August 9

series. The middle and lower flights show a slight skewness with greater deviations on the more moist side.

### C. Correlation Coefficients and Standard Deviations of the Height-Averaged Mixing Ratios

#### 1. Range of Correlation Coefficients Observed

Scanning of the tabulated data presented in Section V shows that the correlation coefficients range from a high of 0.94 to a low of -0.23. The high value applies to the correlation between the two lower layers on one particular day. The highest value for top to bottom is 0.87, found on August 9th. The negative value of -0.23 was found on August 8 - one of the first observing days. This value is accepted with reservations since the negative value probably was generated by poor observational techniques. Later on in the program the flying became more polished and the distances had only small variations. No negative correlation coefficient was observed after the 10th of August. High correlation coefficients of 0.8 or 0.9 occurred at least once each day after the 8th throughout the expedition. After the 10th, 0.21 was the lowest coefficient observed. Hence we can say with confidence that the coefficients vary from 0.9 to 0.2. We cannot definitely state that negative coefficients exist.

#### 2. Vertical Gradients of Correlation Coefficients

When the computed coefficients are averaged according to height we find the following relation. Here again we separate the data into the same two sets.

## Table 6D

### Average Correlation Coefficients

| Set 1 | | Set 2 | |
|---|---|---|---|
| Height Differences | Coefficients | Height Differences | Coefficients |
| 1500 to 1000 | 0.49 | 1200 to 800 | 0.52 |
| 100 to 500 | 0.67 | 800 to 400 | 0.75 |

This table shows that the air lying closer to the surface varies more in unison than the air at the top of the layer. In terms of parcel homogeneity it may be said that the lower air comes closer to the ideal of homogeneous parcels than the upper air.

3. Standard Deviation of the Height-Averaged Mixing Ratios

The individual standard deviations and correlation coefficients were combined to form the standard deviation of the height-averaged mixing ratios as described in Section III. The values of each run are entered in the tables of Section V. The average of all of these values is 0.30 g/kg. Individual samples of the air masses ranged from 0.56 g/kg to 0.14 g/kg. These figures represent the variability of the sub-cloud air column taken as a whole. Individual values of the standard deviation at all levels varied from 0.15 to 1.10 g/kg.

D. Spectral Analysis of the Mixing Ratio Series

As mentioned in Section III it became evident that before the Weckwerth hypothesis could be discussed adequately, information on the contribution of various wavelengths to the variance of the mixing ratio would be required. Hence a program was written for the Recomp II to compute the power spectra of the mixing ratio variations. The spectra for the height averaged mixing ratios have been computed for all the flights. Spectra of the variance at various

each level for 7 flights have been computed so that a comparison between the
levels and the height-averaged spectra could be made. In general the spectra
were computed with lags equal to 25, i.e. 25, 3-second intervals, or 75 seconds.
This corresponds to a little over 10% of the total runs length of 10 minutes or
200 intervals. Lags of 50 were used for the 20-minute runs and for a few of
the short runs for comparison purposes. These lags give first harmonic periods
of 150 and 300 seconds, respectively, and at speeds of 50 m/sec, give wavelengths
of 7.5 km and 15 km. The resolution of the spectral analysis at the longest wave-
lengths is poor partly because of the smoothing process and partly because of
the rapid change of wavelength with harmonic number near the fundamental
harmonic. Thus the correlation of the fundamental period is influenced by the
contribution of power from all periods from the fundamental to infinity. For
the higher harmonics the resolution is much better.

1. Examples of spectra of individual flights

Figures 10-13 present the plots of the spectra of the individual mixing ratios
and height-averaged mixing ratios for 4 different runs. The 6th run of August 10
(280° heading, Figure 10) is of interest because of the occurrance of two rather
large peaks at the 1500-foot level (labelled R4D). One peak occurs at the 6th
harmonic with an amplitude of the variance of 0.0102. Another peak at the 11th
harmonic has an amplitude of 0.0030. The values at the 1000-foot level
(labelled 33T) show a similar peak at the 6th harmonic but much smaller in
amplitude, 0.0011. The 500-foot level (44D) shows no significant maximum at
all but a rather steady decline in amplitude from 0.0286 down to values less
than .0000. Because of the low and negative correlation coefficients between
the mixing ratio values at the different levels, the spectra of the height averaged

mixing ratios is rather featureless except for the concentration of power in the very long wavelengths, which is the most prominent feature of all samples studied during the expedition. The total variance of the height-averaged mixing ratio is about 0.0575 while the spectrum analysis shows that the variance of 0.0481 is contributed by the harmonics less than the 4th, i.e. wavelengths longer than 3.75 km. Thus 84% of the variance is contributed by these long wavelengths.

Run 1, August 11 (100° headings, Figure 11) is a sample showing a small value of the variance, 0.14, and a rather peaked spectrum. The spectrum of the 1200-foot level shows one major peak at the 5th harmonic, $P_5$ ≈ 60 sec, and a minor one at the 13th harmonic, or $P_{13} = 23$ seconds or 1.1 km wavelength. The peak at the 13th harmonic appears at the 800-foot and 400-foot levels with about the same amplitude of 0.0005. The peak at the fifth harmonic does not appear at the lower levels but there is one at the 8th and 9th harmonics. This maximum in variance shows up in the spectra of the 1200-foot level as a bulge on the 5th harmonic peak. Once again 80% of the variance is contributed by the harmonic less than the 4th.

Run 8, August 11 (190° heading, Figure 12) is a sample with unusually large variance at all levels and a height-averaged variance of 0.17. Only very minor peaks are noted in the spectra with 95% of the variance contributed by wavelengths greater than 3.75 km.

Run 3, August 12 (350° heading, Figure 13) is a sample with an interesting distribution of variance at the middle flight level. The top and bottom levels show the usual concentration of power in the long wavelength but the middle run shows a sustained power out to the shorter wavelength. In this case only

27% of the variance is contributed by wavelengths longer than 3.75 while
48% is contributed by wavelengths shorter than 1 km. While this unusual
distribution of power may be partially explained as the random variation
of one sample from the others, this is unlikely since it is a 20 minute
sample and inspection of the height-distance plot of mixing ratio shows that
the water vapor structure was different from most samples. Figure 14
presents a portion of this flight which shows there are many intrusions of
dry air from aloft penetrating the lower air mass in rather narrow fingers.
These intrusions produce the peaks at the 6th, 10th, and 13th harmonics of
the spectra at the 1200-foot level. The intrusions become sharper at the
800-foot level thus producing peaks of variance at higher frequencies. Also,
here the dry air tends to be flanked by more moist air from below. This
phenomenon increases the variance in still higher frequencies, and taken
all together these processes may explain the maintenance of spectral power
to the 50th harmonic. The spectrum of the height-averaged mixing ratio
shows no features except the concentration of power in the long wavelengths.
The washing out of the numerous peaks exhibited in the spectra at the 1200-
and 800-foot levels is the result of the averaging process applied to these
data which are poorly correlated. It is evident from the diagram that a high
degree of correlation exists if account is taken of the slope of the fingers.

2. The mean spectrum of the mixing ratio

From the spectra of the height-averaged mixing ratios for each
flight, an average spectrum has been found and plotted in Figure 15. The
spectrum shows that most of the variance is contained in the long wavelengths.
The numerous peaks of variance that were so conspicuous in the individual

spectra of particular levels are completely smoothed out in this mean spectrum.

### 3. Larger Scales of Mixing Ratio Variation

The concentration of the major portion of the variance in the long wavelengths leads one to wonder about the contribution of even larger scales of motion to variance of the mixing ratio. As the longest airplane runs were 20 minutes or 60 km, no significant analysis of contributions of longer wavelengths could be made from the data obtained on these flights. The only other available source of information concerning mixing ratio in the Bahama region at the time of the expedition was the surface observations made by ships and land stations. These have been compiled in the Northern Hemisphere Data Tabulations of the U.S. Weather Bureau. At 1200 hours GMT nearly all ships at sea take a surface observation from which the mixing ratio can be computed. Using the published surface marine data, charts of the mixing ratios between 20° N and 30° N and 85° W and 65° W were constructed and lines of equal value were drawn. Figure 16 is one example of the charts constructed. It is quite apparent that large scale tongues of moist and drier air occur in some ordered pattern. It will be seen that on the 13th of August our airplane observations were made in the middle of a tongue of moist air. The decrease of mixing ratios to the north and east that were observed from the airplane are clarified and confirmed by this large scale chart. The standard deviations of the ship observations were computed and found to be 1.4 g/kg. While this value is undoubtedly increased by the inherent inaccuracy of ship observations, it is clear from the coherence of the mixing ratio patterns that this value must be about right. This standard deviation corresponds to a variance of about 2.0. When this value is compared to the total variance

observed from the airplane, it is seen that the large-scale variation has an associated variance more than an order of magnitude greater than that associated with the longest wavelengths observed from the airplane and more than two orders of magnitude larger than the variance associated with the smaller wavelengths. From the chart one can make a rough guess that the main contribution comes from wavelengths between 100 km and 1000 km.

4. Histogram of Power Contributions

The contribution to the variance from wavelengths from 1 km to 3.75 km have been summed and tabulated for all of the runs. In addition the contribution of wavelengths from 3.75 km to infinity (or the length of the run), have been summed and tabulated. The results are contained in Tables 6E and 6F. For better visualization histograms of these values have been constructed. They are presented in Figure 17. It is seen that most of the variances summed over 1 to 3.75 km cluster around 0.02 with one case far up the scale at 0.09. The long wavelength histogram shows a clustering around 0.06 with one value of 0.24. The average value of the contribution by the longer wavelengths is 0.06684. The average for the 3.75 to 1 km range is 0.01974.

Table 6E

Contribution to the Variance by two Wavelength Ranges: - ∞ to 3.75 km and

3.75 km to 1 km

Height-averaged Mixing Ratio Expressed in $(g/kg)^2$

| Date | Run Number | ∞ to 3.75 km | 3.75 to 1 km | Direction in relation to wind |
|---|---|---|---|---|
| August 8 | 1 | 0.01889 | 0.01440 | Parallel |
| 8 | 4 | 0.06899 | 0.01376 | " |
| 8 | 5 | 0.03597 | 0.01704 | " |
| 8 | 6 | 0.02760 | 0.01184 | " |

Table 6E Continued

| Date | Run Number | $\infty$ to 3.75 km | 3.75 km to 1 km | Direction in relation to wind |
|---|---|---|---|---|
| August 8 | 7 | 0.01415 | 0.02604 | Parallel |
| 8 | 8 | 0.02908 | 0.01776 | " |
| 8 | 9 | 0.06696 | 0.01441 | " |
| 8 | 10 | 0.05869 | 0.02922 | " |
| | Average | 0.04004 | 0.01815 | " |
| | | | | |
| August 9 | 1 | 0.06086 | 0.02220 | Parallel |
| 9 | 2 | 0.02394 | 0.01568 | " |
| 9 | 3 | 0.20799 | 0.08861 | Cross |
| 9 | 4 | 0.08114 | 0.04416 | " |
| 9 | 6 | 0.07072 | 0.02428 | Parallel |
| | Average | 0.08893 | 0.03899 | |
| | | | | |
| August 10 | 2 | 0.14735 | 0.02073 | Parallel |
| 10 | 3 | 0.04228 | 0.02286 | Cross |
| 10 | 4 | 0.05879 | 0.01852 | " |
| 10 | 5 | 0.07435 | 0.01814 | Parallel |
| 10 | 6 | 0.04812 | 0.00937 | " |
| 10 | 7 | 0.04677 | 0.01990 | Cross |
| 10 | 8 | 0.08404 | 0.02582 | " |
| | Average | 0.07167 | 0.01933 | |
| | | | | |
| August 11 | 1 | 0.01608 | 0.00365 | Parallel |
| 11 | 2 | 0.02187 | 0.00377 | " |
| 11 | 3 | 0.15549 | 0.02081 | Cross |
| 11 | 4 | 0.18613 | 0.02063 | " |
| 11 | 5 | 0.02724 | 0.00841 | Parallel |
| 11 | 6 | 0.03924 | 0.00561 | " |
| 11 | 7 | 0.08656 | 0.00934 | Cross |
| 11 | 8 | 0.14328 | 0.00623 | " |
| | Average | 0.08449 | 0.00980 | |
| | | | | |
| August 12 | 3 | 0.04145 | 0.00874 | Cross |
| 12 | 4 | 0.03550 | 0.00855 | " |
| | Average | 0.03848 | 0.00865 | |
| | | | | |
| August 13 | 2 | 0.12484 | 0.00943 | Parallel |
| 13 | 3 | 0.04772 | 0.01056 | Cross |
| | Average | 0.08628 | 0.01000 | |
| | | | | |
| August 14 | 1 | 0.06937 | 0.02472 | Parallel |
| 14 | 2 | 0.06892 | 0.02052 | " |
| 14 | 3 | 0.04715 | 0.04246 | Cross |
| 14 | 4 | 0.07475 | 0.02793 | " |
| | Average | 0.06505 | 0.02891 | |

| Date | Run Number | ∞ to 3.75 km | 3.75 km to 1 km | Direction in relation to wind |
|---|---|---|---|---|
| August 16 | 1 | 0.07815 | 0.04053 | Parallel |
| 16 | 2 | 0.03001 | 0.00992 | " |
| 16 | 3 | 0.06175 | 0.01854 | Cross |
| 16 | 4 | 0.05153 | 0.01290 | " |
| | Average | 0.05536 | 0.02047 | |
| Average of all flights | | 0.06684 | 0.01974 | |

Table 6F

Contribution to the Variance by two Wavelength Ranges ∞ to 3.75 km and

3.75 to 1 km at Individual Levels

Mixing Ratios expressed in $(g/kg)^2$

| Date | Run Number | Level | ∞ to 3.75 km | 3.75 to 1 km |
|---|---|---|---|---|
| August 8 | 7 | 1500' R4D | 0.05027 | 0.12855 |
| 8 | 7 | 1000' 33T | 0.03065 | 0.03495 |
| 8 | 7 | 500' 44D | 0.07253 | 0.03177 |
| August 9 | 3 | 1500' R4D | 0.72669 | 0.43228 |
| 9 | 3 | 1000' 33T | 0.13178 | 0.04610 |
| 9 | 3 | 500' 44D | 0.13341 | 0.02513 |
| August 10 | 6 | 1500' R4D | 0.20136 | 0.05255 |
| 10 | 6 | 1000' 33T | 0.04044 | 0.00566 |
| 10 | 6 | 500' 44D | 0.08414 | 0.01454 |
| August 11 | 1 | 1200' R4D | 0.03660 | 0.01483 |
| 11 | 1 | 800' 33T | 0.01408 | 0.00947 |
| 11 | 1 | 400' 44D | 0.01706 | 0.00880 |
| August 11 | 4 | 1200' R4D | 0.30764 | 0.07682 |
| 11 | 4 | 800' 33T | 0.13727 | 0.02663 |
| 11 | 4 | 400' 44D | 0.15846 | 0.01790 |
| August 11 | 8 | 1200' R4D | 0.16681 | 0.03041 |
| 11 | 8 | 800' 33T | 0.11798 | 0.01272 |
| 11 | 8 | 400' 44D | 0.15762 | 0.01537 |
| August 12 | 3 | 1200' R4D | 0.03650 | 0.03734 |
| 12 | 3 | 800' 33T | 0.03742 | 0.03385 |
| 12 | 3 | 400' 44D | 0.03461 | 0.02822 |

Table 6F Continued

| Date | Run Number | Level | to 3.75 km | 3.75 to 1 km |
|------|------------|-------|-----------|--------------|
| August 12 | 4 | 1200' R4D | 0.08312 | 0.04075 |
| 12 | 4 | 800' 33T | 0.04007 | 0.01418 |
| 12 | 4 | 400' 44D | 0.05546 | 0.01474 |

E.  Variability of Samples

Before discussing the analyzed data in detail, a check of the sample to
sample and day to day variability of the correlation coefficients, standard
deviations, and spectral distributions will indicate whether the structure of
the atmosphere is relatively constant or subject to extreme variations.
Considering first the variability of the correlation coefficient, it is noted
that this quantity varies from high of 0.94 for $r_{2,3}$ to a low of 0.21 for $r_{1,3}$
if the negative values obtained at the beginning of the expedition are charged
off to poor flight formation.  From Figure 18 the daily averages of the
correlation coefficients appear to be slightly skewed distribution with rather
little scatter about an average value.  From this rather small sample we
conclude that there is no great meteorologically significant day-to-day
variation of the correlation between the mixing ratios at the top and the
bottom of the sub-cloud layer.  This conclusion is valid only for samples
taken in a sequence.  We can say little with assurance about the structure of the
air at a later time from this information, but from our knowledge of the
persistance of weather regimes in the trade wind region it is probable that
small day-to-day variations are usual except during the passage of weather
disturbances.  As for sample to sample variations, it is noted, as commented
before, that the earlier measures of the coefficient suffered from poor alignment
of the airplane and gave a fictitiously large scatter of points about the mean.

Considering the data for August 11 to 16 inclusive, it is noted that the spread of the individual values on any given day is generally larger than the total spread of the daily averages.

From a casual glance it might be concluded that no significant variation of the coefficient has occurred but that the number of points used per sample was too small to obtain a reliable determination of the coefficient. However, the theory of sampling says that correlation coefficients with values greater than 0.2 determined from 200 pairs are significant at a level of less than 1%. Further, the reality of the variation is confirmed by separating the correlation coefficients into cross-wind and parallel-wind runs as indicated on Figure 18. It is noted that two distinct ranges of values exist. For example, the four cross-wind runs of August 11, lie between 0.65 and 0.83, while the four parallel-wind runs lie between 0.26 and 0.64. The probability of such a separation occurring so frequently from chance is very low. A more detailed discussion of this phenomena is presented in the following section.

From previous tabulations it is seen that there is considerable variation of the standard deviation of the mixing ratio from day to day and sample to sample. The individual samples at a given level vary by a factor of about 4 while the height-averaged daily average had a range from only 0.24 to 0.36 g/kg. Tables 6E and 6F show that there is considerable variation in the variance contributed by wavelengths from 3.75 km to 1 km. Considering runs at the 1500' level there is a range from 0.008 to 0.031. Values contributed by the same spectral range of the height-averaged mixing ratio vary over a range from 0.0036 to 0.088. In terms of standard deviation instead of variance the factors are but 10, 2, and 5.

Summing up this discussion of variability we can conclude: (a) that the vertical inhomogeneity varies considerably, but more with direction of sampling relative to the wind than with day to day sampling; (b) the standard deviation shows large variations at the top of the sub-cloud layer, but rather minor day to day and sample to sample variations at the lower layers and (c) the spectral strength in the 3.75 km to 1 km range varies strongly at the upper level, but only moderately at the lower levels. These three conclusions considered together are construed to mean that the structure of the air is moderately constant except for the upper levels of the sub-cloud layer. As the observations were obtained within a period of 8 days, this conclusion can apply only to a similar period of time.

F. The Humidity Structure in Relation to the Woodcock Concept of Oro-
graphic Shower Origin

We now have the analyzed data at hand necessary to determine whether the sub-cloud-air humidity structure is similar to that required by the hypo-thesis of Woodcock (1960). The basic requirement is that the air mass should have a structure such that moist and dry parcels exist which are relatively homogeneous in the vertical and horizontal, and about 1 1/2 km in horizontal extent. These dimensions were determined from Woodcock's observations of showers over Hawaii. He observed that 34 showers passed over one raingauge station while 57 nautical miles of air passed in the same time interval. This sequence of showers embedded in the air mass may be described as a structure having a shower-non-shower variation with an average 3 km wavelength. It is hypothesized that these showers developed from similarly-sized moist and dry parcels which, upon ascending the mountain slope, condensed at different

levels and produced differences in buoyancy. This allowed the moist parcels to rise more rapidly and thus form the nuclei of convective showers.

The problem of checking the present Bahama data against the hypothesis resolves itself into the analysis of the observed time series of mixing ratio values to determine whether parcels in the 1 to 3 km size range have sufficient difference in humidity either individually or collectively to produce the necessary buoyancy differential. Communications engineers, business cycle analysts, and geophysicists have struggled with this problem and have arrived at the conclusion that spectral analysis of time series gives the most useful information concerning the distribution of power among the various frequencies. Tukey (1958) has perfected this technique so that computing machines can be programmed to give very good estimates of the contribution of each harmonic to total variance. Stating the problem in terms of spectral analysis, the testing of the hypothesis requires an estimate of the contribution to the variance of the mixing ratio by harmonics corresponding to wavelengths or parcel sizes between 1 and 4 km. The variance contributed by these wavelengths corresponds to the amplitude of the mixing ratio variations available to be converted into buoyancy differential. The spectra also offer the opportunity to investigate ranges and individual peak and spectrum amplitudes to find the most likely combinations for shower generation.

1. Scale and Magnitude of Horizontal Inhomogeneities

Inspection of all spectra of the height-averaged mixing ratio shows that there is no predominant peak of variance in the 1 to 5 km wavelength range. Rather, the spectra are characterized by low power in the short wavelengths with nearly steady geometric increase in power in the long wavelengths. The

spectra of the individual levels do, however, show considerable power in peaks within the 1 to 4 km range. The top level possesses peaks with the greatest variance.

To study this problem quantitatively several values of the contribution to the variance by certain wavelengths are collected in column 2 of Table 6G. These values represent means and extremes of particular significance.

### Table 6G

### Vertical Motions Scaled from the Malkus-Witt Convective Model

| Wave-length | Variance | Standard Deviation | Temperature Difference | Vel. Scale Factor | Time Scale Factor | Vertical Disp. | Time |
|---|---|---|---|---|---|---|---|
| km | $(g/kg)^2$ | g/kg | °C | | | m | min |
| (a) Values from mean of all spectra | | | | | | | |
| 7.5 | 0.024 | 0.156 | 0.25 | 1.79 | 3.5 | 1250 | 21 |
| 3.75 | 0.0099 | 0.100 | 0.16 | 1.00 | 3.16 | 635 | 19 |
| 2.5 | 0.0044 | 0.066 | 0.11 | 0.68 | 3.1 | 420 | 19 |
| 1.9 | 0.0025 | 0.05 | 0.08 | 0.50 | 3.1 | 310 | 19 |
| 1.5 | 0.0014 | 0.037 | 0.06 | 0.39 | 3.2 | 250 | 19 |
| 0.75 | 0.0002 | 0.015 | 0.025 | 0.18 | 3.5 | 125 | 21 |
| (b) Summation of contributions from 1 to 3.75 km | | | | | | | |
| 2.38 | 0.0197 | 0.14 | 0.23 | 0.96 | 2.1 | 400 | 12 |
| (c) Maximum value in 1 to 3.75 km range of height-averaged mixing ratio spectra (Run No. 3 August 9, 1960) | | | | | | | |
| 3.75 | 0.04786 | 0.218 | 0.35 | 1.48 | 2.1 | 620 | 12 |
| (d) Maximum value in 1 to 3.75 km range of individual spectra (Run No. 3 August 9, 1960, 1500', cross-wind) | | | | | | | |
| 3.75 | 0.175 | 0.42 | 0.67 | 2.04 | 1.5 | 930 | 8 |

Column 2 of this table presents (a) the variance associated with the listed wavelengths of the mean of all the spectra, (b) the sum of the variances contributed by all the wavelengths from 1 to 3.75 km, (c) the maximum value of the height-averaged mixing ratio spectra between 1 and 3.75 km, and (d) the maximum value of the individual spectra. It is seen that the variance contributed by wavelengths in these different categories varies by 4 orders of magnitude. To evaluate the effectiveness of these various combinations in producing convection nuclei we must first change the variance to standard deviations and then estimate the temperature differences produced by forcing the air up a mountain slope. Column 3 gives the standard deviation. To determine the temperature differences generated by the differential condensation resulting from the upslope motion of parcels of different mixing ratios an adiabatic diagram was used. From such a diagram it is seen that if two parcels of air with mixing ratios of $\bar{q} + 0.14$ g/kg and $\bar{q} - 0.14$ g/kg (corresponding to a standard deviation of 0.14 g/kg) are lifted until the drier parcel is at 100% relative humidity, then the more moist parcel will have had 0.09 g/kg of its water vapor condensed and its temperature would be 0.23°C warmer than the drier parcel. Column 4 of Table 6G gives the temperature differences generated in this manner from the standard deviations given in Column 3. The temperature differences range from 0.025°C to 0.67°C.

Now we are faced with the question "Will a significant vertical circulation be established between pairs of parcels with the temperature differences and dimensions listed in Table 6G?" A definite reliable answer is not available since nobody has studied parcels with exactly these dimensions and character-istics. Malkus and Witt (1959) have studied by numerical calculation the life

history of convective cells originating from stationary 300 meter parcels whose temperature differed from the neutral environment by 0.5°C. Such parcels developed strong organized vertical circulation after two minutes. In the case of a parcel in contact with the ground the region of maximum temperature difference rose at a rate of 1 m sec$^{-1}$ between the 2nd and 3rd minutes and then the velocity decreased. After 6 minutes the region of maximum temperature had risen 200 m. In the case of a parcel with its base elevated above the ground, the region of maximum temperature rose 300 m in 5 minutes. We can attempt to scale these results to fit the present sizes and temperature differences between the model and the case of airflow up a slope. Wind shear, sharp turbulence, initial vertical velocities, and differential upslope motion are all unknown and may have a large but unknown effect.

The model velocities and displacements may be scaled to the present sizes by dimensional analysis. The velocities may be scaled making use of the equation, $w = (gbR)^{1/2}$, where g is the acceleration of gravity, b is the buoyancy which is proportional to the temperature differences, and R is the radius of the parcel. The radius of the parcel in this case is considered to be 1/4 of the wavelength. The time of development of the cell is scaled according to $T = (R/gb)^{1/2}$. These scale features are found for each case and listed in columns 5 and 6. Using these scale features we find the scaled vertical displacements of the region of maximum temperature and the time to achieve this displacement. These estimates are listed in columns 7 and 8.

It is quite apparent that some of these combinations have a very good chance of producing regions of increased temperature that will rise relative

to their neighbors and probably produce a shower cell. Others such as the 0.75 km wavelength parcels of the mean spectra probably would not survive the turbulence and shears of the upslope wind for 20 minutes. A parcel represented by the summation of the variance contributed by the wavelengths between 1 and 4 km would survive to form a shower. The uncertainty in this case is whether a parcel composed of so many contributing wavelengths would organize as a single parcel with a variance equal to the sum. The height-averaged contribution by the 3.75 km wavelength of Run No. 3, August 9, 1960 appears to be ample to form a shower cell. The most promising case of all is that of the 1500' level of Run No. 3, August 9, 1960. In this case there was a strong peak in the harmonic corresponding to a 3.75 km wavelength which would be capable of producing a parcel 0.67°C warmer than the drier parcels. As this corresponds to the 'up in the air bubble' of Malkus and Witt, such a bubble would rise 930 m in 8 minutes. Such a rapid rise would almost certainly produce a shower.

The analysis of the moisture data shows that there are variations in the humidity of the atmosphere of such a size and magnitude that many seem to be capable of producing shower cells. There are other mechanisms such as gravitational waves, flow instabilities, and random turbulent gusts that also might produce shower nuclei. No attempt has been made to evaluate the probabilities of buoyant cell production by other mechanisms but they must be evaluated and compared to the differential moisture hypothesis before the most likely mechanism can be determined.

G. Cross-Wind and Parallel-Wind Relationships

It is of interest to look for systematic differences between the correlations

and standard deviations observed on flights with a course parallel to the wind and with a course perpendicular to the wind. Many studies both theoretical and observational have been made of convection and turbulent flow and the resulting cellular patterns that are set up in either the atmosphere or the ocean (Brunt, 1941; Faller, unpublished). Cloud rows oriented at different angles to the wind have been observed by many observers on many occasions. hence it seems useful to study the humidity distribution in the sub-cloud layer for evidence of some systematic motion. The best method of doing this is to compare the values of the deviations and correlations observed during cross-wind flights with those observed during flights parallel to the wind.

1. Correlation Coefficient Relations

The averages of the correlation coefficients for all days and all heights have been found for the cross-wind runs and the parallel-wind runs. They are nearly identical; 0.587 for the cross-wind and 0.578 for the parallel-wind runs. This fact rules out any simple spiral circulation with an axis exactly parallel or perpendicular to the wind direction as an average condition. Looking at Figure 18 it is seen that on individual days the cross-wind correlation coefficients are separated distinctly from the parallel-wind coefficients. If we exclude the first three days data from this discussion because of the poor flight formations, we see that the remaining days show a puzzling relationship. On the 11th the cross-wind runs have coefficients separated from the parallel-wind coefficients and which have a greater value. On the 14th, however, a similar separation occurs but the cross-wind coefficient now has a lower value. On the 16th the two ranges of coefficients

overlap with the cross-wind coefficients having the smaller range as is usually the case. The interpretation of these results cannot be conclusive for lack of supplementary data. However, it is consistent with a helical velocity structure of the air with the mean axes of the helices at different angles to the wind. Thus on August 11 the data might be interpreted as indicating helices nearly parallel to the wind. On the 13th and 14th helices more nearly perpendicular to the wind might be indicated. Other days might indicate a 45° alignment, or horizontal isotropy.

### 2. Standard Deviation Relationships

The averages of the standard deviations also show a weak relation between the cross-wind and parallel-wind differences. The two values of 0.38 and 0.35 g/kg for the averages of the individual values. The average of the standard deviation of the height-averaged mixing ratio is 0.35 for the cross-wind case to 0.27 for the parallel-wind case. The individual values for August 11, show a strong relation for the first 4 runs with the cross-wind runs having deviations more than twice the parallel-wind runs. However, in subsequent runs the cross-wind deviations decreased and the parallel-wind deviations increased so that the last runs showed an insignificant difference. It is concluded that no consistant or long-lived difference in the organization of convective cells in the atmosphere exists although short duration organization seems to exist.

### 3. Spectral Power Relations

Since the standard deviations just discussed include the effects of mean horizontal gradients in the mixing ratio, it is well to study the spectral analysis data for cross-wind and parallel-wind relations. Table 6E shows

that in all cases save one the cross-wind variances contributed by wavelengths from 3.75 to 1 km are larger than the parallel-wind variances.

H. Relation of Statistical Parameters to Wind Speed

Many relationships of the various parameters to wind speed and wind shear were looked for but none of them showed any significant relationship. Rather than describe each investigation in detail and present the scatter diagram that was plotted, and found inconclusive, the relationship investigated will be listed only.

1. Mixing ratio versus wind speed

2. Average standard deviation versus wind speed

3. Cross-wind parallel-wind deviation differences versus wind speed

4. Correlation coefficients versus wind speed

5. Cross-wind parallel-wind correlations versus wind speed

6. Cross-wind parallel-wind deviation differences versus wind shear.

## References

Blackman, R. B. and J. W. Tukey, 1958: The measurement of power spectra. Dover Publications, Inc., New York. 190 pp.

Brunt, David, 1941: Physical and Dynamical Meteorology. Cambridge University Press. 428 pp.

Bunker, A. F., B. Haurwitz, J. S. Malkus, and H. Stommel, 1949: Vertical Distribution of temperature and humidity over the Caribbean Sea. Pap. Phys. Ocean. and Meteor. Vol. XI, No. 1, 82 pp.

Bunker, A. F. and K. McCasland, 1954: Description and installation of meterological equipment aboard Navy PBY-6A, 46683. WHOI Ref. No. 54-82 Unpublished report to Office of Naval Research.

Faller, Alan, 1961: The instability of the laminar Ekman boundary layer. Unpublished manuscript. Woods Hole Oceanographic Institution.

Malkus, Joanne, 1958: On the structure of the trade wind moist layer. Pap. Phys. Ocean. and Meteor. Vol. XII, No. 2, 47 pp.

Malkus, J. S. and G. Witt, 1959: The evolution of a convective element: a numerical calculation. Rossby Mem. Vol., Oxford Univ. Press and Rockefeller Inst. Press N. Y. 425-439 pp.

Woodcock, A. H., 1960: The origin of trade-wind orographic shower rains. Tellus. Vol. 12, No. 3, 315-326 pp.
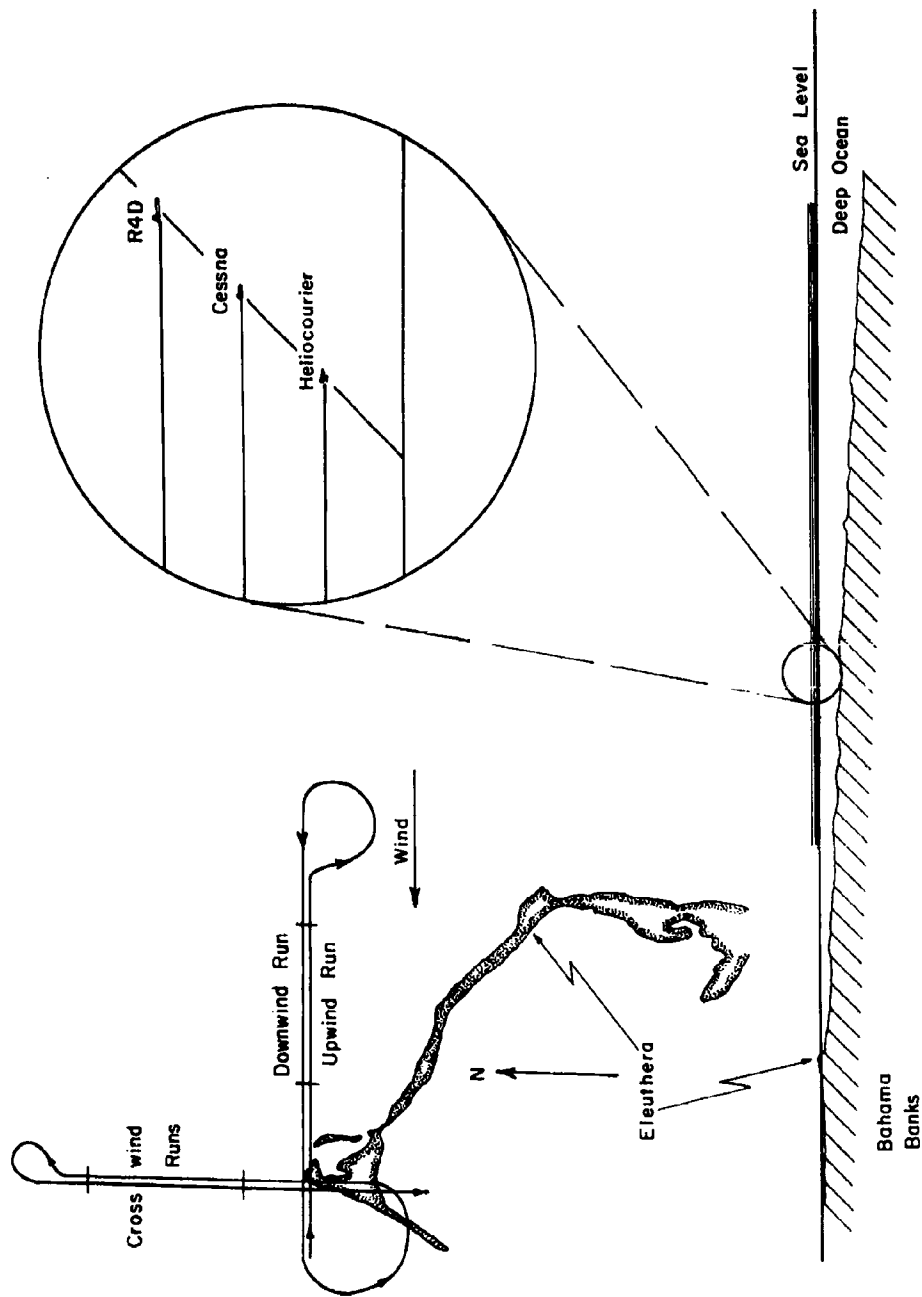
FIGURE 1.  Diagram and chart showing vertical section of atmosphere
studied, alignment of airplanes, and courses flown.
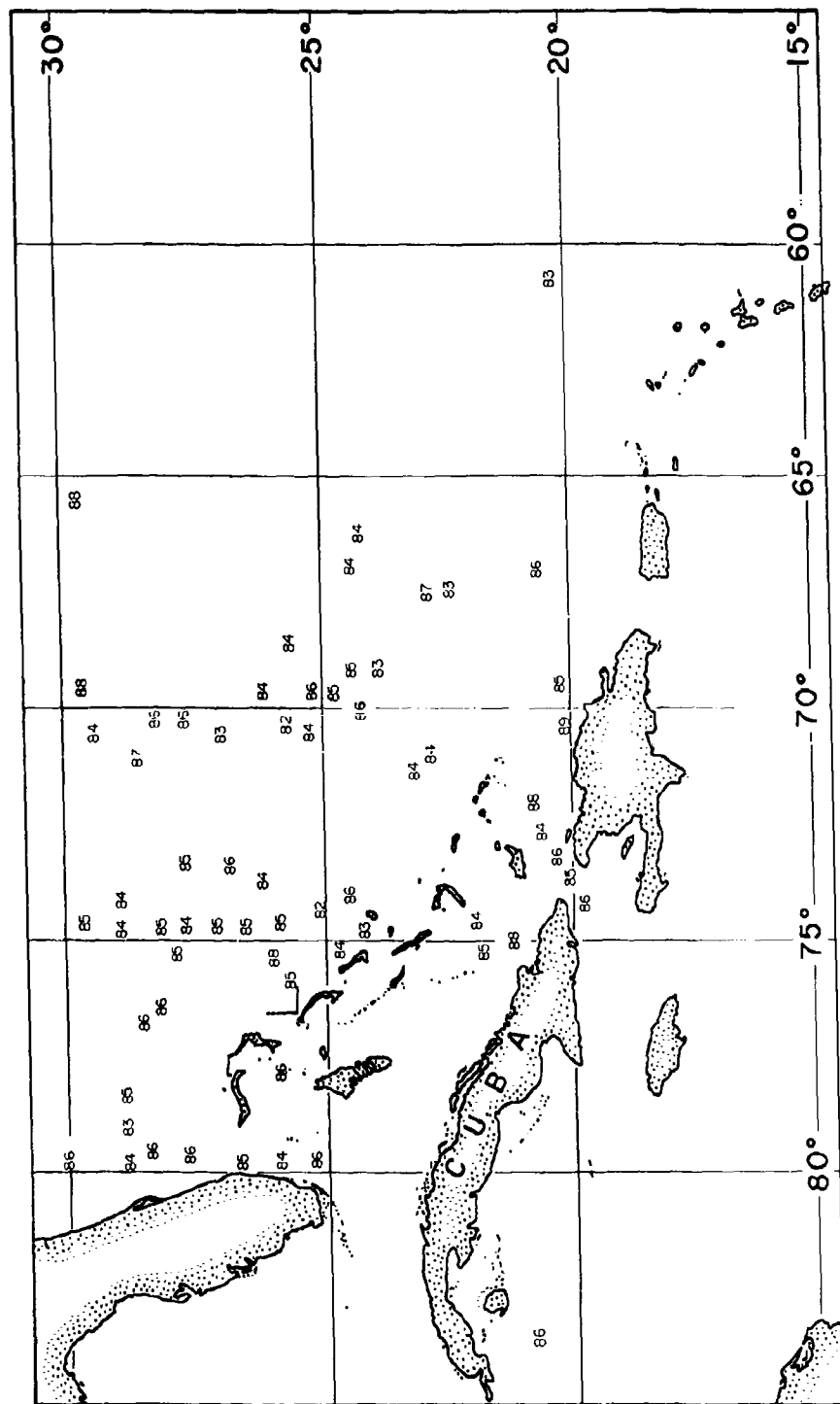
FIGURE 2. Sea temperature chart. Ship observations taken between August 8 and 16,1960 are entered in degrees Fahrenheit. The line segments indicate the flight paths executed.
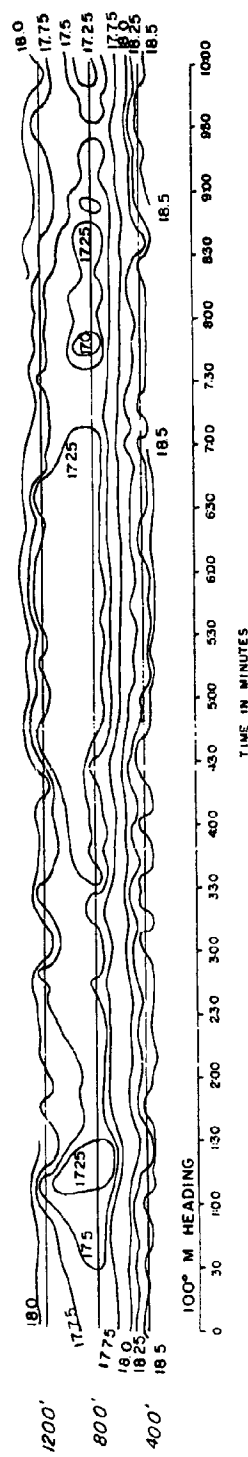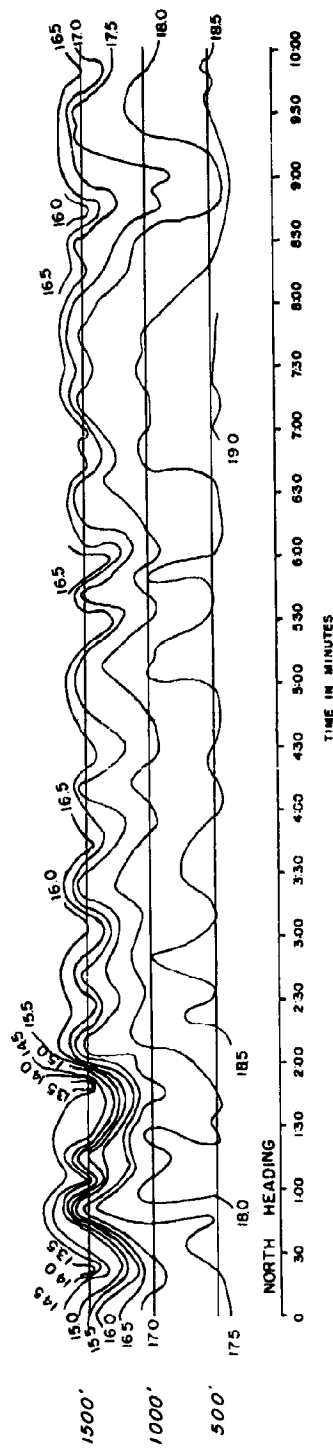
FIGURE 3. Mixing ratio cross sections. Top: Run #3, August 9. Example of high variability, $\bar{v}_{123} = 0.56$ g/kg. Bottom: Run#1, August 11. Example of low variability $\bar{v}_{123} = 0.14$ g/kg.
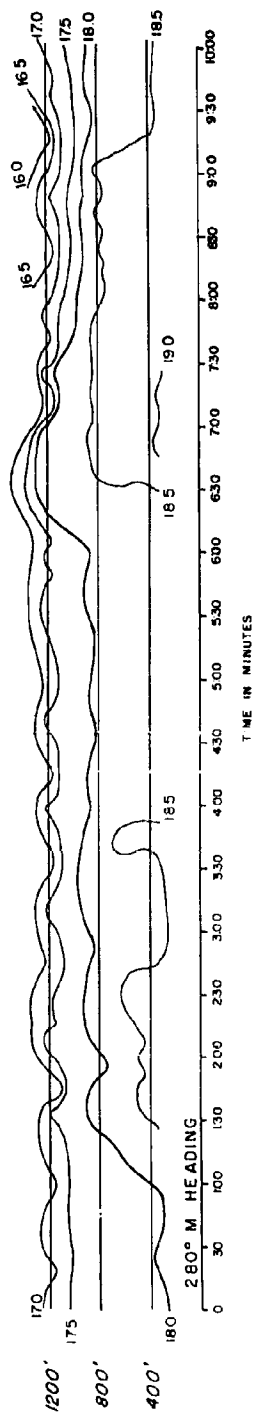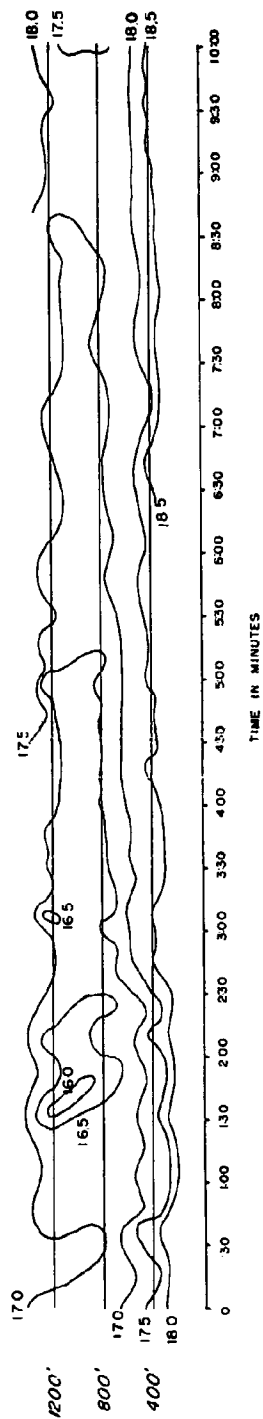
FIGURE 4. Mixing ratio cross sections. Top: Run#8 August 11. Example of high correlation coefficient, $r_{1,3} = 0.83$. Bottom: Run#6, August 10. Example of low correlation coefficient $r_{1,2} = 0.07$.
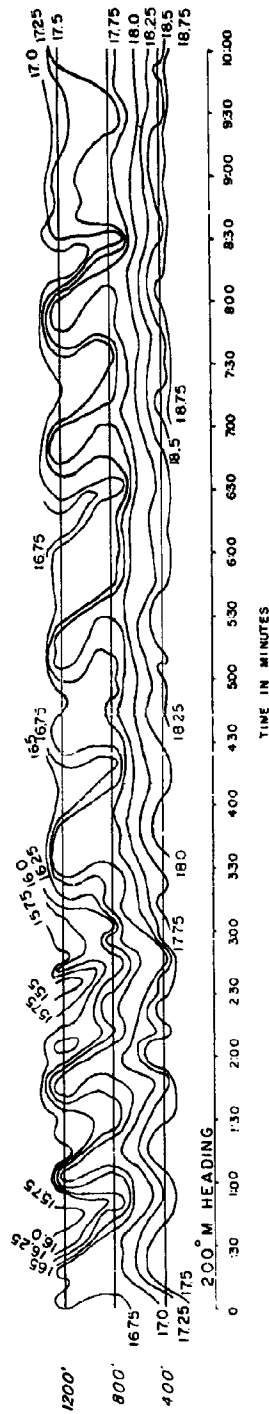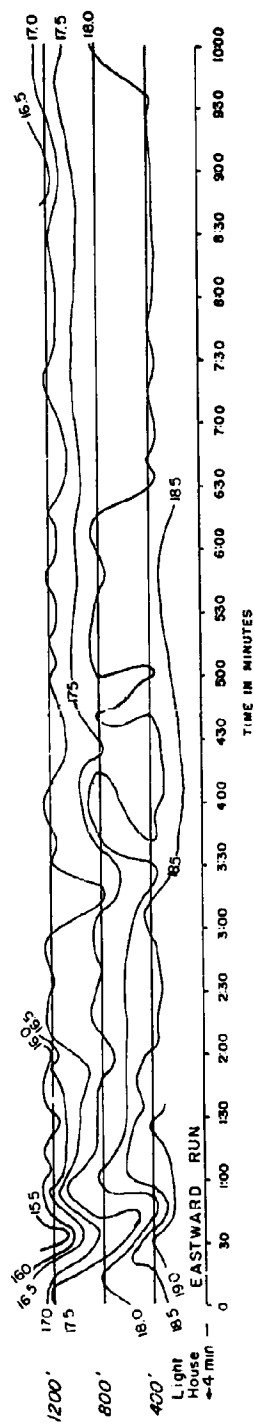
Figure 5. Mixing ratio cross sections Top: Run#7, August 8/ Example of negative correlation coefficient $r_{2,3} = -0.23$. Bottom: Run #4, August 11. Example of regular variations.
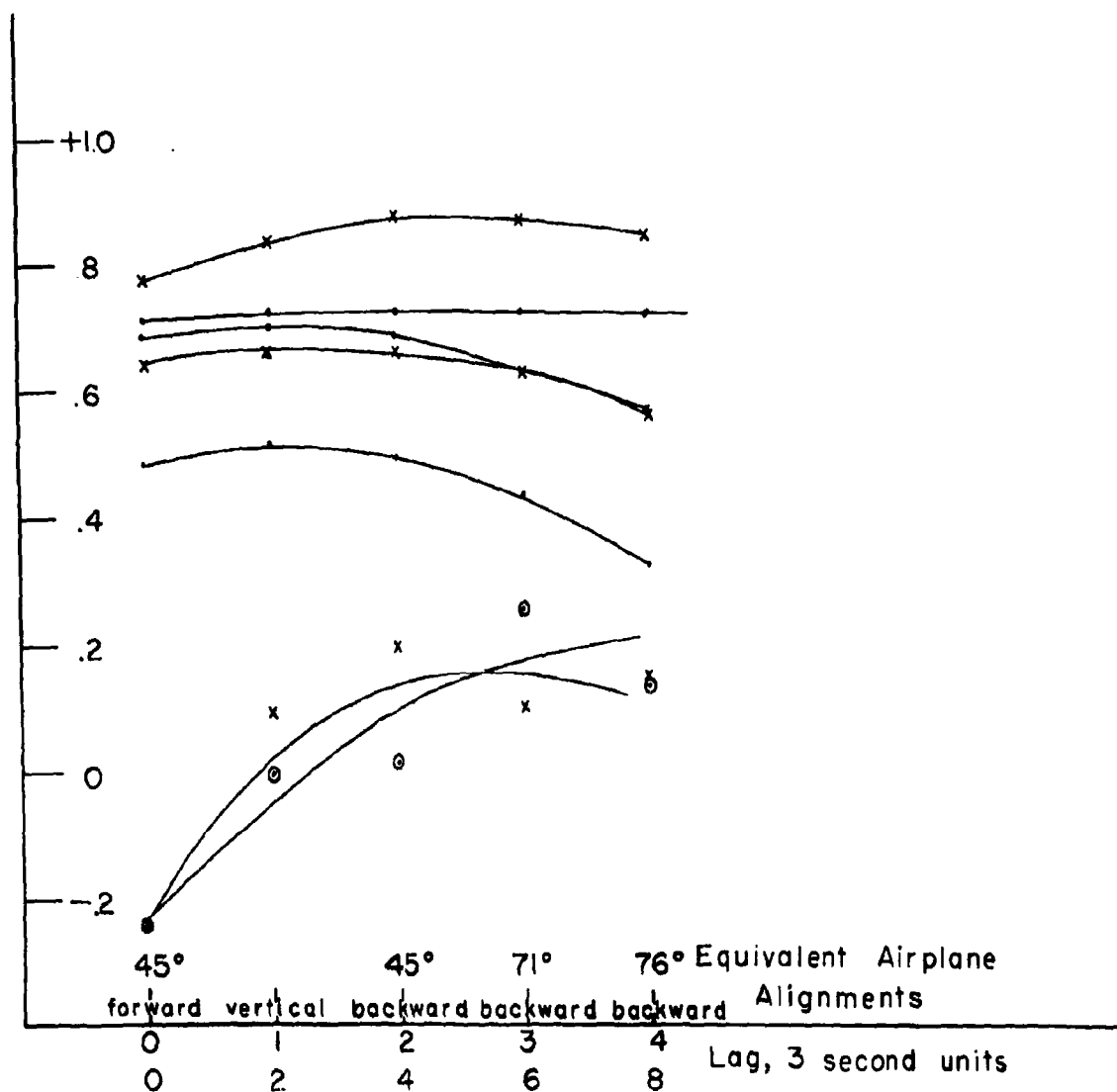
FIGURE 6. Correlation coefficients for equivalent airplane alignments.
Coefficients were computed with top levels lagged to simulate
different vertical alignments of the airplanes.
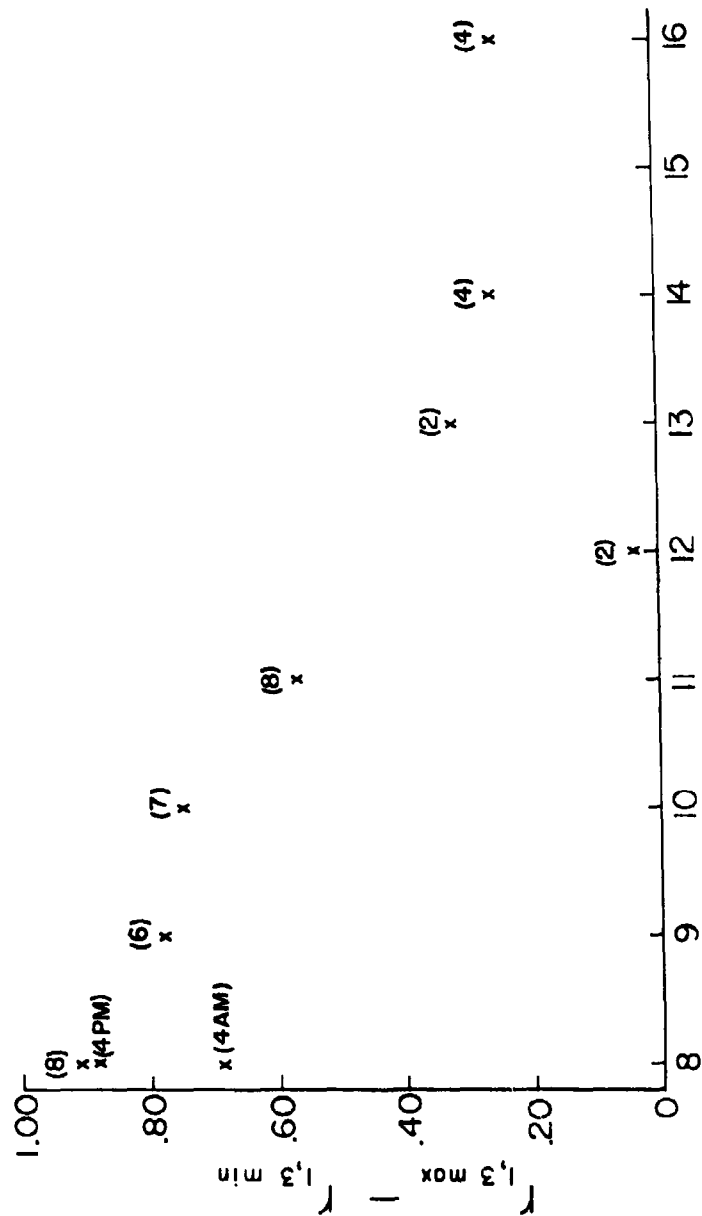
FIGURE 7. Maximum range of correlation coefficients observed on given days.
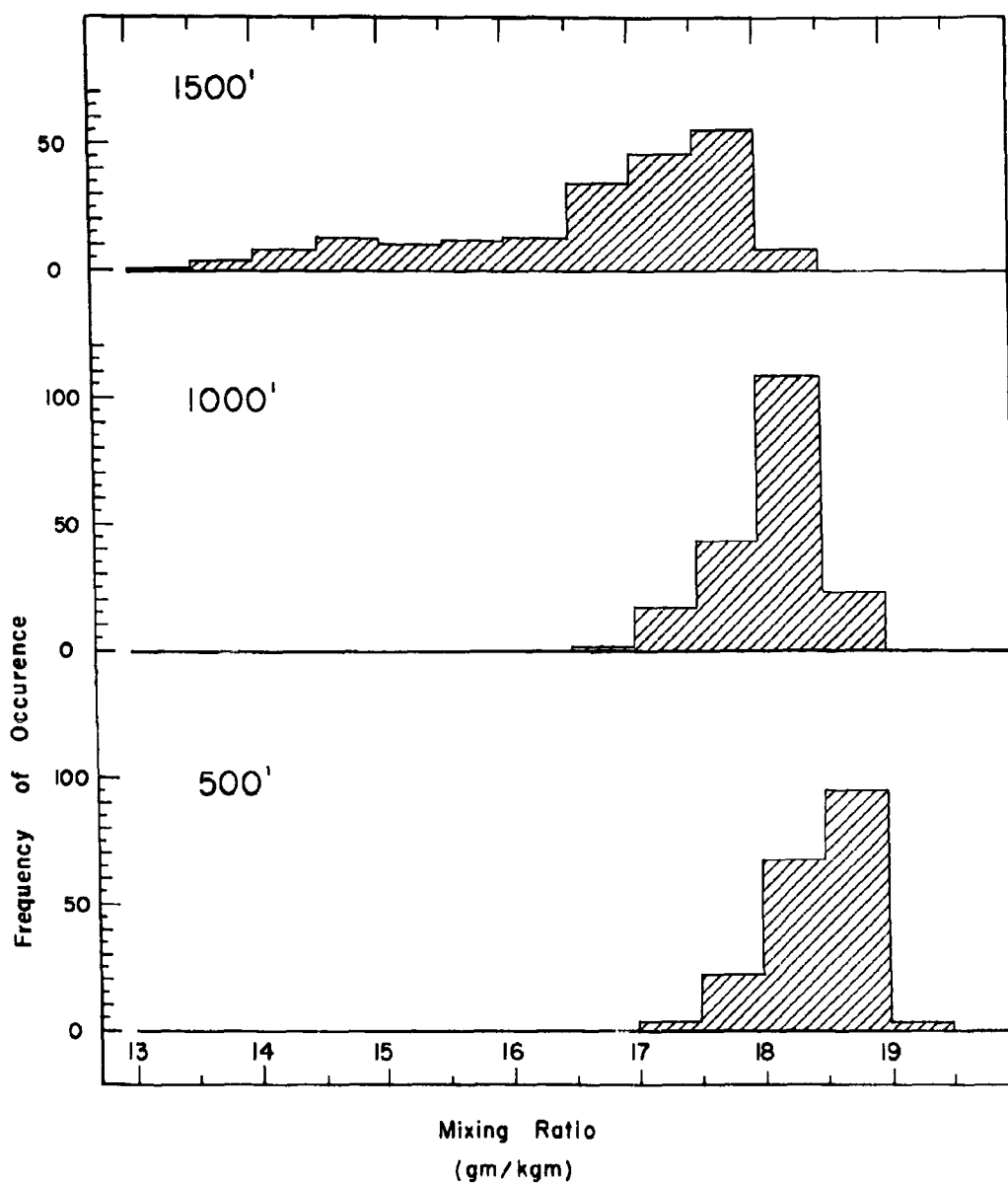
Figure 8.   Histograms of mixing ratios observed at three levels of
Run #3, August 9, show the skewness of the distributions.
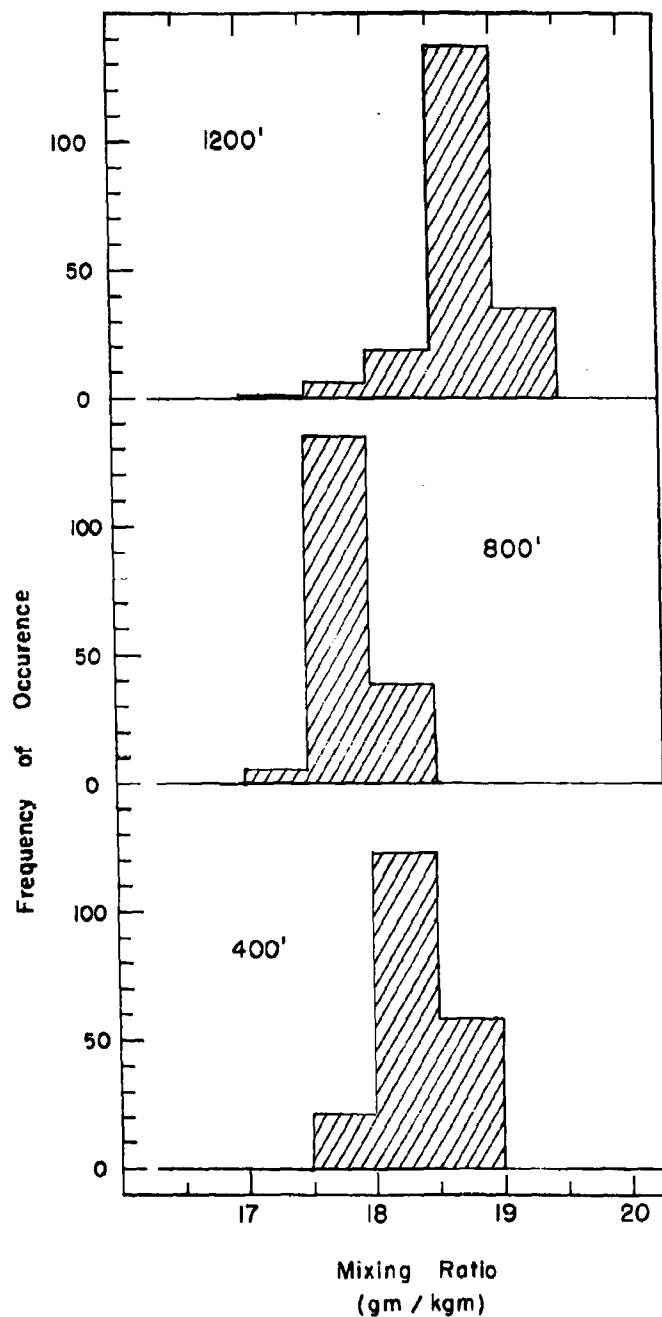
FIGURE 9. Histograms of mixing ratios observed at three levels of Run #2, August 16, 1960, show the lack of a pronounced skewness of the distributions.
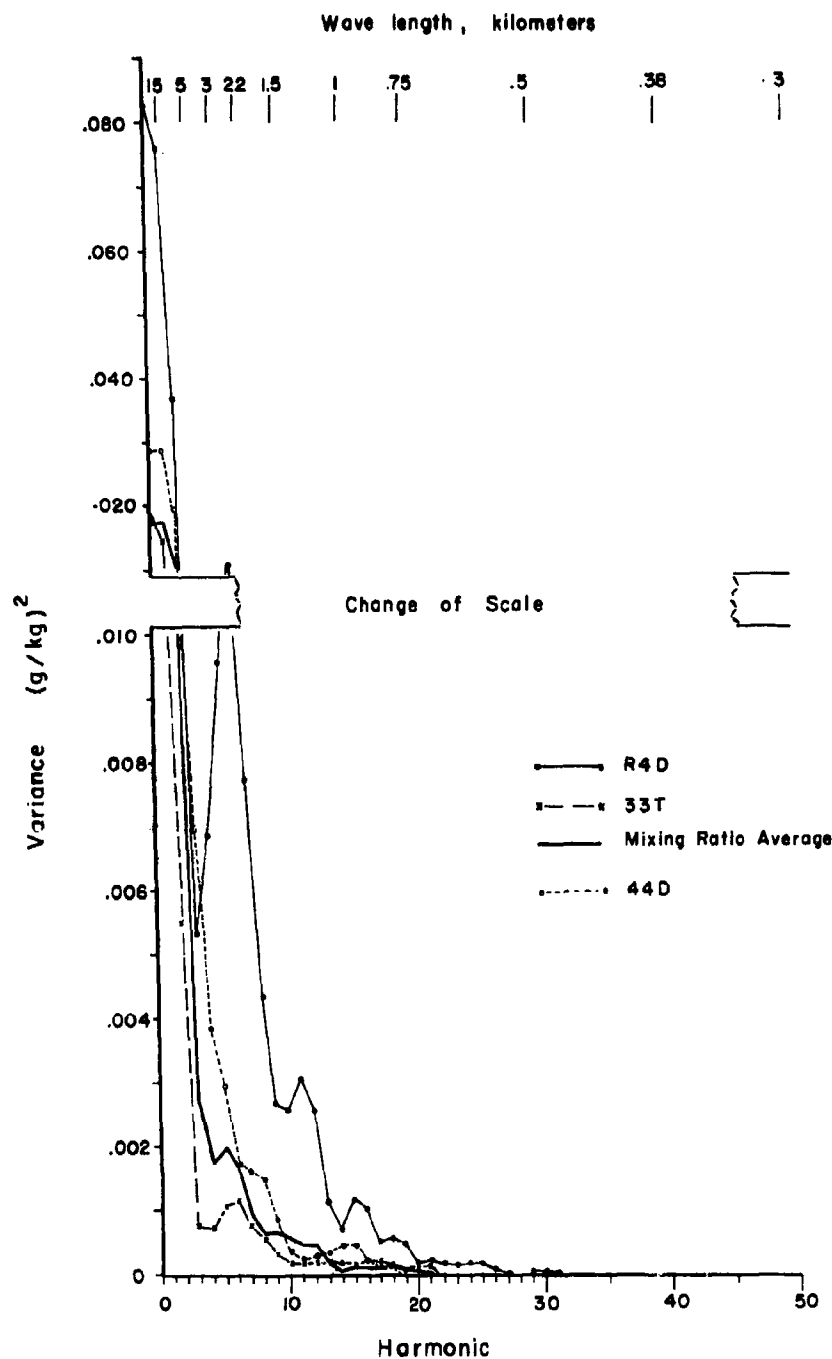
FIGURE 10. Spectral analysis of Run #6, August 10. The contribution to
the variance of the mixing ratio by each harmonic for each
level and the height-averaged mixing ratio is presented.
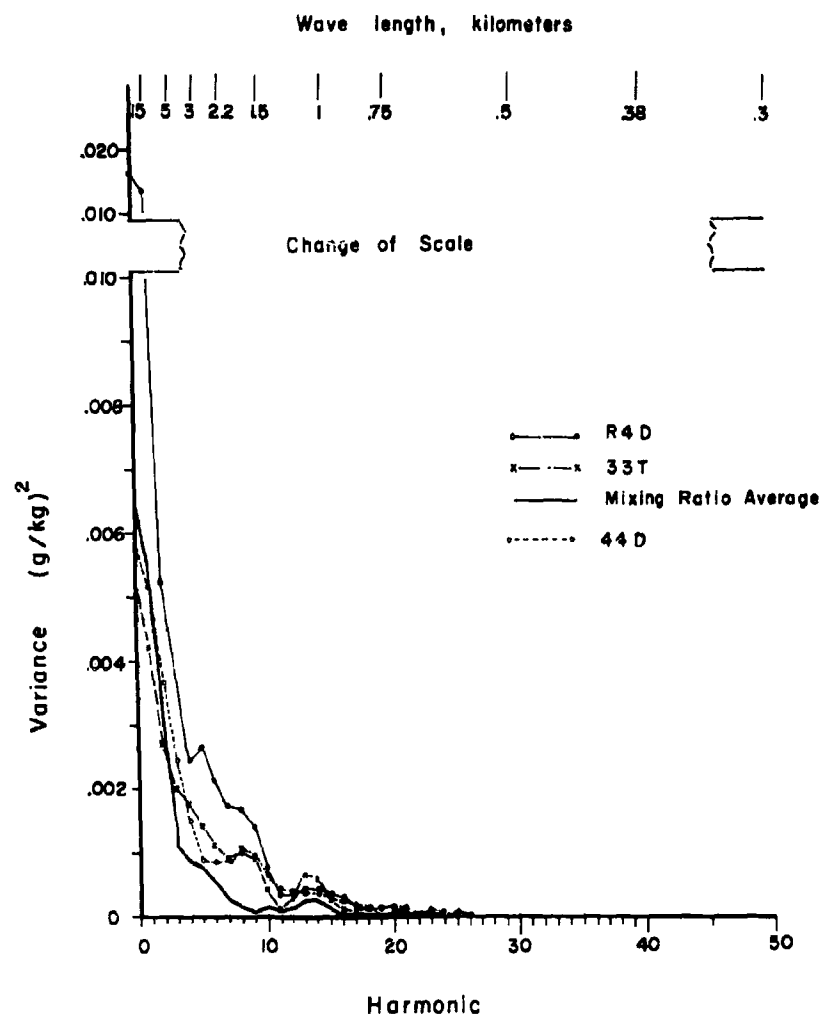
FIGURE 11. Spectral analysis for Run#1.August,1960. The contribution
to the variance of the mixing ratio by each harmonic for
each level and the height-averaged mixing ratio is presented.
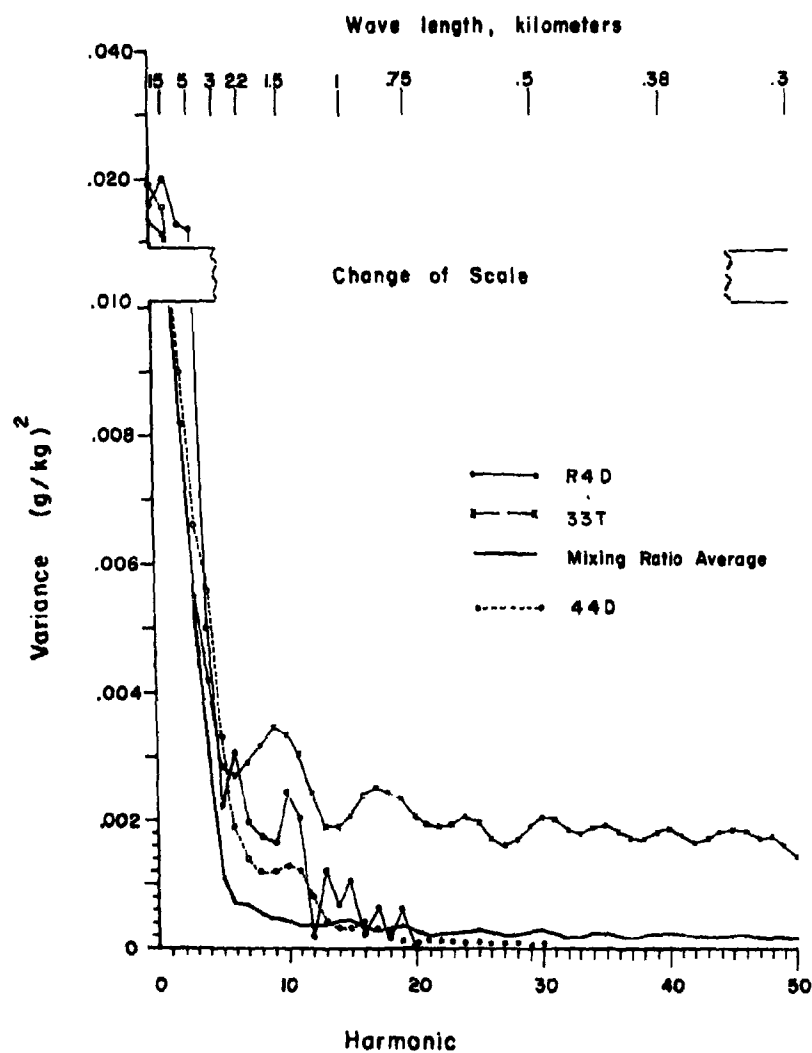The period of the fundamantal harmonic is 300 seconds.
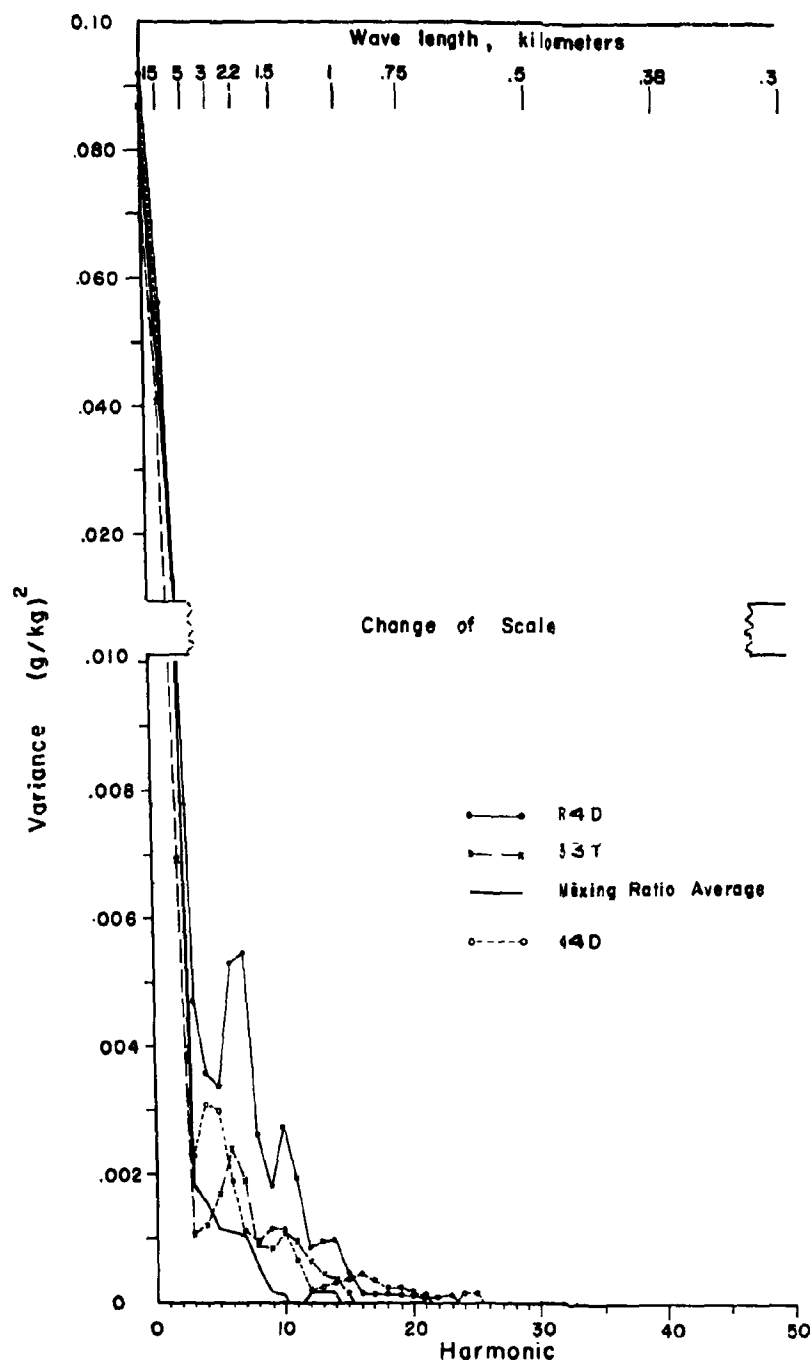
FIGURE 12. Spectral analysis of Run #8, August 11, 1960. The contribution
to the variance of the mixing ratio by each harmonic for each
level and the height-averaged mixing ratio is presented.
The period of the fundamental harmonic is 300 seconds.

FIGURE 13. Spectral analysis of Run#3,August 12,1960. The contribution
to the variance of the mixing ratio by each harmonic for
each level and the height-averaged mixing ratio is presented.
The period of the fundamental harmonic is 300 seconds.
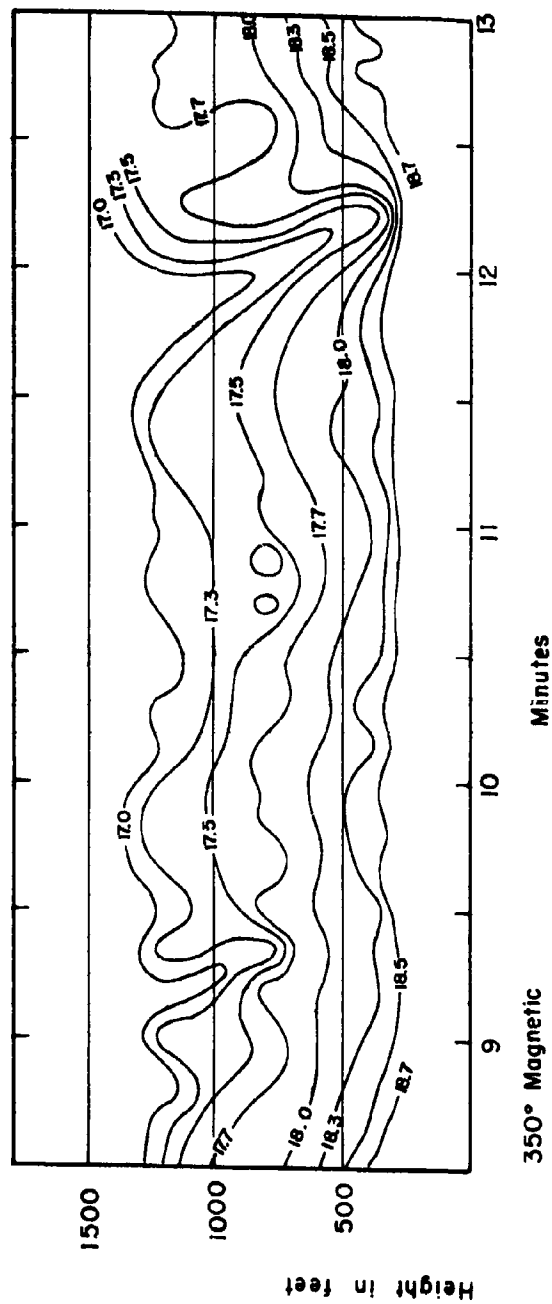
FIGURE 14. Vertical cross section of mixing ratio observed on August 12, 1960, Run #3 showing intrusions of dry air into sub-cloud region.
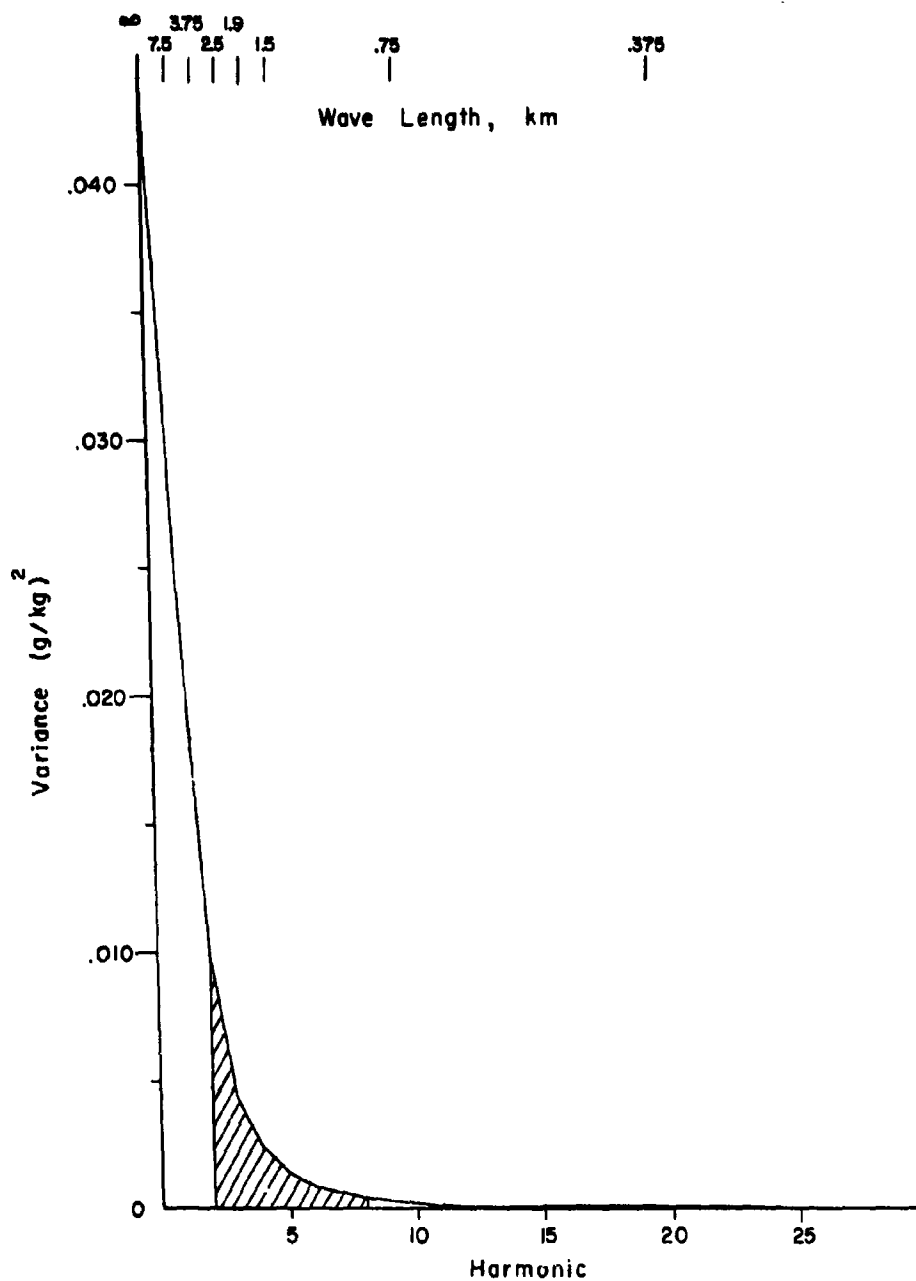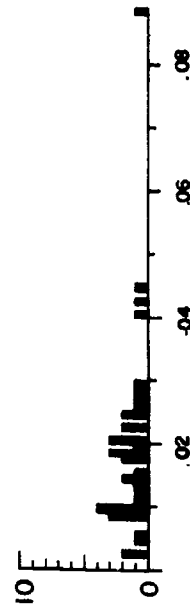
FIGURE 15. Mean spectrum of the mixing ratio. Area of hatching represents
contribution to the variance by wavelengths from 1 km to 3.75
km. The period of the fundamental harmonic is 150 seconds.

FIGURE 16. Chart of surface mixing ratios observed from ships at 1200 GCT August 13, 1960.

FIGURE 17. Histograms of variance of the mixing ratio contributed by wavelengths from ∞ to 3.75 km and 3.75 km to 1 km.
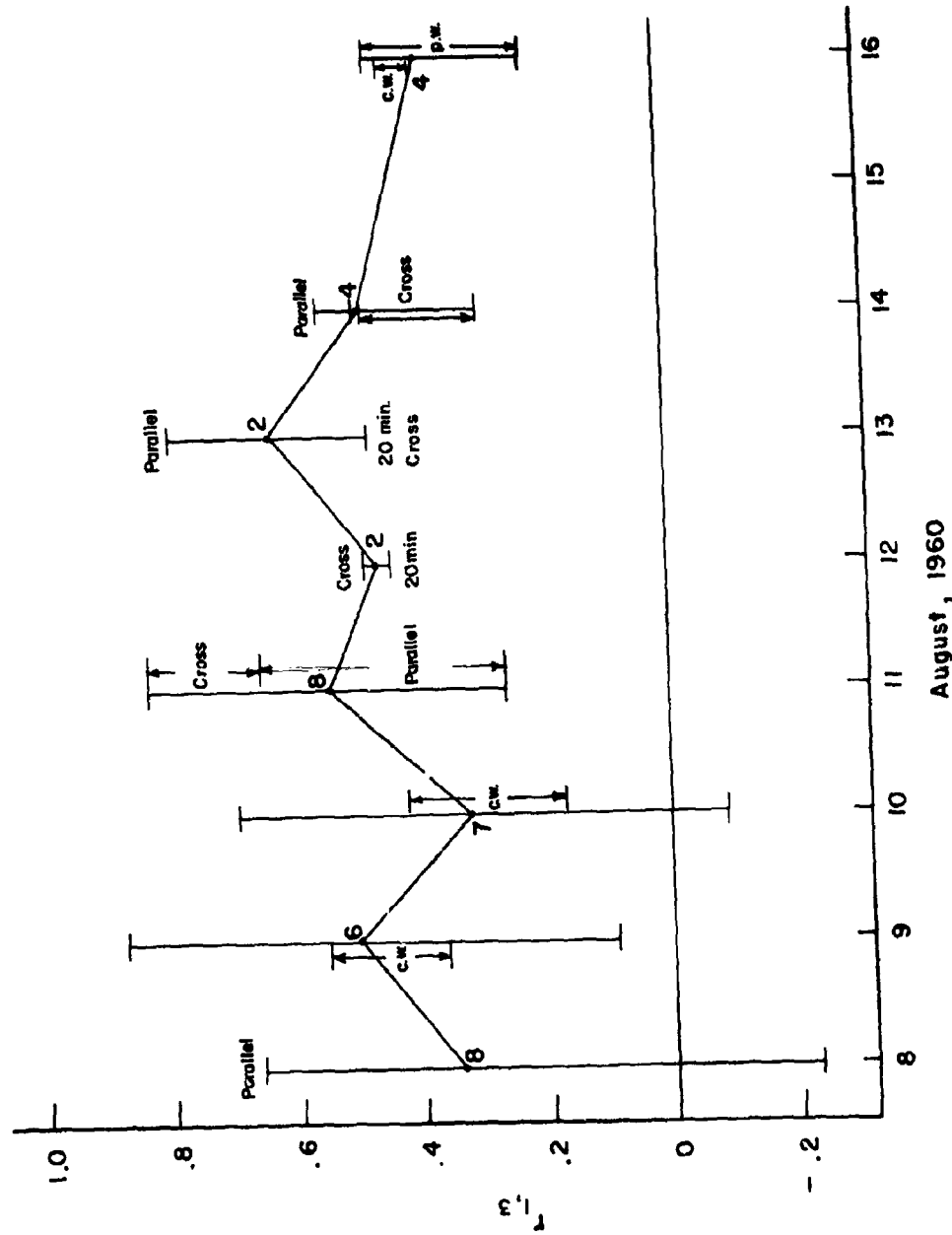
FIGURE 18. Daily range of correlation coefficients. Ranges of coefficients observed on parallel-wind runs and cross-wind runs are indicated by connecting lines and arrowheads.